Neutron stars as dark matter detectors

Ariel Zhitnitsky[*]

Department of Physics and Astronomy, University of British Columbia,
Vancouver, V6T 1Z1, British Columbia, Canada

It has been known for quite some time that neutron stars (NSs) can play a role in dark matter (DM) detectors due to many unique features of NSs. We apply these (previously developed) ideas to a specific form of the DM when it is represented by a composite object, rather than by a local fundamental field (such as WIMPs). To be more precise we consider the so-called axion quark nuggets (AQN) dark matter model, when the "nonbaryonic" dark matter in fact is made of quarks and gluons which are in dense quark phase (similar to the old idea of the Witten's strangelets). We argue that the interaction of the AQNs with NSs material may lead to many profound observable effects, which are dramatically different from the conventional picture when DM particles are represented by WIMPs. In particular, we argue that the AQNs may serve as the triggers for the magnetic reconnection to heat the NSs' surface. This effect may strongly alleviate (or even completely remove) the observed inconsistencies between the predicted and observed surface temperatures for many old NSs. This heating mechanism is always accompanied by the hard x-ray emission, which may serve as an indicator of the proposed mechanism.

I. INTRODUCTION

It has been known for a long time that the dynamics of the neutron stars (NSs) can be modified by the influence of dark matter (DM) particles [1–13]. Furthermore, it has also been known that the basic properties of the DM particles can be strongly constrained by considering DM-NS interactions. In particular, the conventional cooling pattern of NSs can be modified due to the capturing and consequent annihilation of the DM particles [1–3]. There are many other processes which could potentially become observable as a result of interaction of the DM particles with a very dense NS environment. We refer to several original papers [1–14] devoted to analyses of many possible physical phenomena which could result from such DM-NS interactions. This is obviously a very broad area of research, and we refer to the recent paper [15] for review on this topic.

In the present work we consider a specific model for the DM which is dramatically different from the conventional paradigm when DM particles are assumed to be new (yet to be discovered) fundamental weakly interacting massive particles (WIMPs). Before we elaborate on this specific form of DM represented by macroscopically large nuclear density composite objects made of quarks and gluons, we detour with an overview of the most important features the DM particles must satisfy.

Observational precision data gathered during the last quarter of the century have guided the development of the so-called concordance cosmological model ΛCDM of a flat universe, $\Omega \simeq 1$, wherein the visible hadronic matter represents only $\Omega_B \simeq 0.05$, a tiny fraction of the total energy density, see recent review [16], and interesting historical comments [17]. Most of the matter component of the Universe is thought to be stored in some unknown kind of cold dark matter, $\Omega_{DM} \simeq 0.25$. The largest contribution $\Omega_\Lambda \simeq 0.70$ to the total density is cosmological dark energy with negative pressure, another mystery which will not be discussed in the present work.

There is a fundamental difference between dark matter and ordinary matter (aside from the trivial difference dark vs visible). Indeed, DM played a crucial role in the formation of the present structure in the Universe. Without dark matter, the Universe would have remained too uniform to form the galaxies. Ordinary matter could not produce fluctuations to create any significant structures because it remains tightly coupled to radiation, preventing it from clustering, until recent epochs. On the other hand, dark matter, which is not coupled to photons, would permit tiny fluctuations to grow for a long, long time before the ordinary matter decoupled from radiation. The required material is called cold dark matter, and the obvious candidates are the WIMPs of any sort which are long-lived, cold,

[*]arz@phas.ubc.ca

and weakly interacting with visible hadronic material. The key parameter which enters all the cosmological observations is the corresponding cross section σ to mass M_{DM} ratio which must be sufficiently small to play the role of DM as briefly mentioned above, i.e.

$$\frac{\sigma}{M_{\mathrm{DM}}} \ll 1 \ \frac{\mathrm{cm}^2}{\mathrm{g}}, \tag{1}$$

and WIMPs obviously satisfy to the criteria (1) to serve as DM particles. However, the WIMP framework which has been the dominant paradigm for the last 40 years has failed as dozens of dedicated instruments could not find any traces of WIMPs though the sensitivity of the instruments had dramatically improved by many orders of magnitude during the last decades.

In the present work we consider a fundamentally different type of the DM which is in the form of the dense macroscopically large composite objects, similar to Witten's quark nuggets [18–20]. The corresponding objects are called the axion quark nuggets (AQN) and behave as *chameleons*: they do not interact with the surrounding material in a dilute environment, such that the AQNs may serve as proper DM candidates as the corresponding condition (1) is perfectly satisfied for the AQNs during the structure formation when the ratio $\sigma/M_{\mathrm{AQN}} \lesssim 10^{-10}$ cm^2 g^{-1}. However, the same AQNs become strongly interacting objects in a sufficiently dense environment, such as planets and stars. The interaction of AQNs with a NS's environment also dramatically deviates from conventional WIMP-NS interactions. Therefore, many observable consequences discussed previously [1–15] are dramatically modified as a result of strong interactions of the AQNs with a NS's environment.

In the present work we address a single but very important question related to a NS's cooling scenario: why is the observed surface temperature of many old NSs well above the conventional theoretical predictions? The proposed answer is that this excess of heating is the result of the AQN-NS interaction, which is the topic of the present work.

Before we present our arguments supporting this claim we briefly overview several previously proposed heating mechanisms in Sec. II which could in principle generate some extra heat and could potentially answer the question formulated above. We argue, however, that standard astrophysical sources are very unlikely to be responsible for the observed excess of heating and there must be some unconventional sources of heat to explain the anomalies in observations.

The rest of our presentation is organized as follows. In Sec. III we overview the basic features of the AQN model relevant for the present studies. In Sec. IV we formulate the main lessons to be learned from our previous studies of the AQN interactions with the solar corona. We apply these ideas to AQN-NS interaction in Sec. V where we argue that DM in the form of the AQNs may serve as the triggers igniting the large explosive events (due to magnetic reconnections, similar to solar flares). The dynamics of magnetic reconnection as the heating source of NSs is elaborated in detail in Secs. VI and VII. In Sec. VIII we argued that the study of the hard x ray's emission from NSs (using magnificent seven stars as an example) can serve as the indicator of the proposed heating mechanism. We list our basic results in Sec. IX where we also mention some other manifestations and observational consequences of the AQN framework. Many technical details on physics of the magnetic helicity $\mathcal{H}$ powering the magnetic reconnection are discussed separately in Appendix A.

II. POSSIBLE HEATING MECHANISMS OF OLD NSs

We start with a brief overview of the minimal cooling theory; see original paper [21] and recent review [15]. The observations in general are in very good agreement with the minimal cooling paradigm when the neutrino emission from the core dominates at early times ($t \lesssim 10^5$ yr). The photon emission from the surface dominates at $t \gtrsim 10^5$ yr, when the neutrino emission rate gets highly suppressed and the NS cools down. As a result, it is expected that the NS surface temperature rapidly decreases to $T_s^\infty \lesssim 10^4$ K at $t \gtrsim 10^6$ yr, which represents a generic consequence of the minimal cooling theory.[1]

However, some recent studies of old pulsars apparently are inconsistent with this canonical cooling theory, see e.g. [22–24] for the references on the numerous original results. These results suggest that some new sources of heating must be operational to explain the observed surface temperature being higher than expected.[2] There are many subtle points in such "measuring" of the surface temperatures, see footnote 2 with comments, such that all recorded values should be taken with a grain of salt and with some scepticism.

Nevertheless, this phenomenon when "measured" surface temperature is much higher (than naively expected temperature) is very common and generic, and it is unlikely that it can be entirely explained by combination of the

---

[1]The T_s^∞ in this work is defined as the observed surface temperature at infinity. To be more precise, the T_s^∞ is defined as $T_s^\infty = T_s \sqrt{1 - \frac{2\,\mathrm{GM}}{\mathrm{R}}}$, where T_s is the surface temperature in its local reference frame, while R and M are the radius and the mass of the NS.

[2]One should emphasize that there are numerous subtle points in "measuring" of the NS's temperature as it is influenced by a nonthermal component. Furthermore, there are often the hot spots localized at the poles which also may dramatically modify the measuring of the average temperature of the NS. The author is thankful to the anonymous referee for pointing out on these subtleties in measuring of the average temperatures.

uncertainties mentioned above and in footnote 2. In fact, a higher (than expected) temperature is observed for very different stars with very different properties such as period, age, magnetic field, etc., which supports the claim that canonical cooling is far from being sufficient to explain all of the observations. In principle one could do modeling to separate different radiation mechanisms to extract more precisely the average value of temperature for a given NS. These questions are well outside the scope of the present work and we refer to the papers already mentioned [22–24] for review, for our arguments which follow any precise values of the measured temperatures are not essential. Our arguments are based on a qualitative observation that in a large number of cases the observed temperature is higher than predicted, and we propose that some accompanied effects (not directly related to measurement of the surface temperature, see Sec. VIII) may test our proposal.

Many mechanisms which could potentially heat the old NS have been suggested. In particular, it includes magnetic field decay, DM accretion, crust cracking, vortex creep, rotochemical heating, to name just a few; see [22] for a brief review and references. It was argued previously that some NSs which are slightly older than $\sim 10^6$ yr can be explained by some (or the combination) of these mechanisms. However, there are still many cases when suggested mechanisms are not capable to explain the data; see details below.

In the rest of this section we critically overview some of the most promising mechanisms suggested previously. We also identify some cases when these mechanisms still fail to explain the observed data. Precisely this dramatic failure in explanation of the observed data was the main motivation for the present work to suggest a novel heating mechanism which has the potential to explain the observed anomalies. First, we start with a brief overview of previously suggested heating mechanisms, see e.g. [22].

A. Rotochemical heating

The rotochemical heating is considered to be the most promising heating mechanism [22–24]. The basic idea is that the chemical equilibrium is altered when the rotation of the star is slowing down. The relaxing to the new equilibrium state enforces the emission of photons which eventually heat the surface. There is a number of uncertainties in the estimates which could be sensitive to many parameters of the models, such as the gap, the EoS, or initial conditions for young pulsars expressed in terms of the initial period P_0. The fitting of all of these parameters in principle allows one to explain the observed surface temperatures of ordinary pulsars. However, in many cases this mechanism fails to explain the observed surface temperatures.

For example, the T_s^∞ of the so-called magnificent seven stars cannot be explained by this mechanism with reasonable changes of the parameters, see Fig. 3 in [23]. Another set of examples includes the old pulsars with $t \gtrsim 10^9$ yr with $T_s^\infty \sim 10^5$ K, see e.g. the two first rows in Table 1 in [23]. Such old and warm pulsars obviously cannot be explained by the rotochemical heating mechanism with any reasonable modifications of the parameters; see Figs. 3 and 4 in [23]. There are many similar cases when the observed temperatures T_s^∞ dramatically exceed the theoretical estimates, and we shall not discuss all of these cases in detail.

For the purposes of the present work the most important outcome of these estimates is that the rotochemical heating obviously could be efficient and operational in many cases. However, there are also many cases when it dramatically fails, which implies that (a) there is no unified and simple mechanism which explains the observed data, and (b) there must be some other mechanisms which could also be important and which become especially pronounced at later times of the NS's evolution.

B. Magnetic field decay

Another mechanism of heating which was widely discussed in the literature in the past is heating due to the magnetic field decay; see e.g. review in [22]. It is common and a generally accepted view that the magnetic field cannot play a role of heating for relatively old stars with $t \gtrsim 10^6$ yr. Nevertheless, we opted to present the conventional arguments (on irrelevance of the magnetic field) below as the AQN-induced mechanism of heating of NSs, to be introduced later in Sec. V, which will be based precisely on transferring the magnetic energy to heat. We will show in Sec. VII where and why the conventional arguments (on irrelevance of the magnetic field) fail for this specific AQN model.

The basic idea of the naive estimate is to assume that the decaying magnetic field strength $\mathcal{B}$ transfers its energy to the surface on the timescale t. In this case one can equalize the luminosity L of the NS with decreasing magnetic energy in the entire NS, i.e.

$$L = 4\pi R^2 \sigma T_s^4 \approx \frac{4\pi R^3}{3} \cdot \frac{\langle \mathcal{B}^2 \rangle}{8\pi} \cdot \frac{1}{t}. \tag{2}$$

The corresponding numerical estimate [22] suggests that the required magnetic field to explain the observations with $T_s \sim 10^5$ K is too high. Indeed,

$$\sqrt{\langle \mathcal{B}^2 \rangle} \sim 10^{13} \cdot \sqrt{\frac{t}{10^7 \text{ yr}}} \cdot \sqrt{\frac{10 \text{ km}}{R}} \cdot \left(\frac{T_s}{10^5 \text{ K}} \right)^2 \text{ G}, \tag{3}$$

which is much higher than the observed magnetic field in classical pulsars $\sim 10^{11}$ G and millisecond pulsars $\sim 10^8$ G. As a result of this simple estimate the magnetic field as the source of heating was largely ignored in the literature, in spite of the fact that the magnetic field potentially represents an enormous energy reservoir.

There are many subtle elements in this oversimplified estimate because many assumptions being incorporated into (2) and (3) may not be justified. Indeed, in the estimate above it was assumed that the magnetic field is dominated by a large scale dipole, which may not be the case because very different configurations may be the dominant contributors to the magnetic energy. In fact, precisely the enormous magnetic energy reservoir will play a key role in heating of the NS within the AQN framework as we argue in this work. The relevant configuration though is not represented in terms of a simple large scale dipole configuration, as assumed in (3), but rather is represented by complicated helical fields which will be the source of the heating as we argue below in Sec. VII. Furthermore, the relevant timescale entering the right-hand side of estimate (2) will be very different from (t) entering (2) which dramatically modifies the oversimplified conventional estimate (3).

C. Dark matter accretion

We want to mention one more heating mechanism which occurs due to DM accretion. This mechanism was also widely discussed in the literature. Similar to the previous case reviewed above in Sec. II B, it was also thought that DM cannot play any essential role of heating for a NS with $T_s \sim 10^5$ K as maximum temperature which could be achieved by DM accretion cannot exceed $T_s \approx 3 \times 10^3$ K for any reasonable parameters; see e.g. review [22]. Therefore, this mechanism could potentially play a role but for very old stars of age $t \gtrsim 10^8$ yr.

The basic idea of the estimate is to observe that the maximum possible accretion rate onto a NS is given by

$$\dot{M} \approx \rho_{\mathrm{DM}} \pi b_\infty^2 v_\infty, \tag{4}$$

where ρ_{DM} is the local DM density in the vicinity of the NS, and the velocity v_∞ and impact parameter b_∞ are defined at very large distances from the NS. Assuming that the entire amount of energy of the DM particles is released in the form of heat, one can infer that

$$\dot{M}c^2 \lesssim 5 \times 10^{22} \; \frac{\mathrm{erg}}{\mathrm{s}}, \tag{5}$$

which is many orders of magnitude smaller than the radiation from the NS with temperature $T_s \sim 10^5$ K. Indeed,

$$L = 4\pi R^2 \sigma T_s^4 \approx 7 \times 10^{28} \left(\frac{T_s}{10^5 \; \mathrm{K}}\right)^4 \frac{\mathrm{erg}}{\mathrm{s}}, \tag{6}$$

which is 6 orders of magnitude higher than the DM accretion heating mechanism can provide according to estimate (5). As a result of this simple estimate, it has been concluded that the dark matter accretion mechanism may

play a role only for very old stars of age $t \gtrsim 10^8$ yr, and it can be safely ignored for younger NSs with temperature $T_s \gtrsim 10^5$ K.

The irrelevance of the DM physics for a NS with temperature $T_s \gtrsim 10^5$ K was based on the canonical assumption that the DM particles are some kind of fundamental (yet to be discovered) new particles in the form of WIMPs. Precisely this type of DM particles was previously considered in the literature in the context of DM-NS interaction [1–15].

In contrast with this WIMP framework, we are advocating the AQN framework where DM is in the form of the dense macroscopically large composite objects, similar to Witten's quark nuggets [18–20], as mentioned in Sec. I. In this case the macroscopically large AQNs can play the dual role: they obviously can inject the energy directly, similar to WIMPs, in which case the constraint (5) holds (with minor numerical modifications).

However, the same AQNs could also play the role of the triggers which can initiate and ignite magnetic reconnections such that the enormous magnetic energy reservoir stored in the NS's atmosphere and crust can heat the NS's surface as will be discussed in Sec. V. Precisely this dual role of the AQNs dramatically modifies the conclusion of Sec. II B on irrelevance of the magnetic field as a possible heating mechanism of a sufficiently old NS.

Before we present the main elements on the AQN-induced heating mechanism of the NS in Secs. V–VII, we have to make a detour to introduce the basics of the AQN framework in Sec. III and the lessons to be learned from similar processes (though in dramatically different environments) of interactions of AQNs with the solar corona in Sec. IV.

III. THE AQN DARK MATTER MODEL

We overview the fundamental ideas of the AQN model in Sec. III A, while in Sec. III B we list some specific features of the AQNs relevant for the present work.

A. The basics

As we already mentioned the AQN construction in many respects is similar to Witten's quark nuggets, see [18–20]. This type of DM is "cosmologically dark" as a result of smallness of the parameter (1) relevant for cosmology. This numerically small ratio scales down many observable consequences of an otherwise strongly interacting DM candidate in the form of the AQN nuggets.

There are several additional elements in the AQN model in comparison with the older well-known and well-studied theoretical constructions [18–20]. First, there is an additional stabilization factor for the nuggets provided by the axion domain walls which are copiously produced during the QCD transition. This additional element helps us to alleviate a number of problems with the original Witten's

TABLE I. Basic properties of the AQNs adopted from [33]. The parameter κ is introduced to account for possible deviation from geometric value πR^2 as a result of ionization of the AQNs due to interaction with environment. The ratio $\Delta B/B \ll 1$ implies that only a small portion ΔB of the total (anti)baryon charge B hidden in the form of the AQNs get annihilated during big bang nucleosynthesis, cosmic microwave background, or postrecombination epochs (including the galaxy and star formation), while the dominant portion of the baryon charge survives until the present time.

Property	Typical value or feature
AQN's mass $[M_N]$	$M_N \approx 16 \text{ g}(B/10^{25})$ [30]
Baryon charge constraints $[B]$	$B \geq 3 \times 10^{24}$ [30]
Annihilation cross section $[\sigma]$	$\sigma \approx \kappa \pi R^2 \simeq 1.5 \times 10^{-9} \text{ cm}^2 \cdot \kappa (R/2.2 \times 10^{-5} \text{ cm})^2$
Density of AQNs $[n_{\text{AQN}}]$	$n_{\text{AQN}} \sim 0.3 \times 10^{-25} \text{ cm}^{-3}(10^{25}/B)$ [30]
Survival pattern during BBN	$\Delta B/B \ll 1$ [31,32,34,35]
Survival pattern during CMB	$\Delta B/B \ll 1$ [31,34,36]
Survival pattern during postrecombination	$\Delta B/B \ll 1$ [29]

model. In particular, a first-order phase transition is not a required feature for nugget formation as the axion domain wall (with internal QCD substructure) plays the role of the squeezer.

Another problem of the old construction [18–20] is that nuggets likely evaporate on the Hubble timescale. For the AQN model, this is not the case because the vacuum-ground-state energies inside (the color-superconducting phase) and outside the nugget (the hadronic phase) are drastically different. Therefore, these two systems can co-exist only in the presence of an external pressure, provided by the axion domain wall, which is an inevitable feature of the AQN construction. This should be contrasted with the original model [18–20], which is assumed to be stable at zero external pressure. This difference has dramatic observational consequence relevant for the present work; the Witten's nugget will turn a NS into the quark star if it hits the NS. In contrast, a matter type AQN will not turn an entire star into a new quark phase because the quark matter in the AQNs is supported by external axion domain wall pressure, and therefore, can be extended only to relatively small distance $\sim m_a^{-1}$, which is much shorter than the NS's size.

Finally, the nuggets can be made of *matter* as well as *antimatter* during the QCD transition. The presence of the antimatter nuggets in the AQN framework is an inevitable and direct consequence of the $\mathcal{CP}$ violating axion field which is present in the system during the QCD time. As a result of this feature, the DM density, Ω_{DM}, and the visible density, Ω_{visible}, will automatically assume the same order of magnitude densities $\Omega_{\text{DM}} \sim \Omega_{\text{visible}}$ irrespective of the parameters of the model, such as the axion mass m_a. This feature represents a generic property of the construction [25] as both components, the visible and the dark, are proportional to one and the same fundamental dimensional constant of the theory, the Λ_{QCD}.

We refer to the original papers [26–29] devoted to the specific questions related to the nugget's formation, generation of the baryon asymmetry, and survival pattern of the nuggets during the evolution in the early Universe with its unfriendly environment. We also refer to a recent brief review article [30] which explains a number of subtle points on the formation mechanism and survival pattern of the AQNs during the early stages of the evolution, including the cosmic microwave background (CMB), big bang nNucleosynthesis (BBN), and recombination epochs.

The only comment we would like to make here is that in this work we take the agnostic viewpoint, and assume that such nuggets made of *antimatter* are present in our Universe today irrespective to their formation mechanism. This assumption is consistent with all presently available cosmological, astrophysical, and terrestrial constraints as long as the average baryon charge of the nuggets is sufficiently large as we review below.

We conclude this brief review subsection with Table I which summarizes the basic features and parameters of the AQNs. An important point here is that only a small portion $\Delta B \ll B$ of the total (anti)baryon charge B hidden in the form of the AQNs gets annihilated during the long evolution of the Universe. The dominant portion of the baryon charge survives until the present time. Independent analyses in [31,32] also support our original claims as cited in Table I that the antiquark nuggets survive the BBN and CMB epochs.

We draw the AQN structure on Fig 1, where we use typical parameters from Table I. There are several distinct length scales of the problem: $R \sim 10^{-5}$ cm represents the size of the nugget filled by dense quark matter with total baryon charge $B \sim 10^{25}$ in colour superconducting phase. A much larger scale $R_{\text{DW}} \sim m_a^{-1}$ describes the axion domain wall (DW) surrounding the quark matter. The axion DW has the QCD substructure surrounding the quark matter, which has typical width of order $R_{\text{QCD}} \sim 10^{-13}$ cm. Finally, there is always an electrosphere which represents a very generic feature of quark nuggets, including Witten's original construction. In case of antimatter nuggets, the electrosphere comprises the positrons. The typical size of the electrosphere is order of 10^{-8} cm; see below.
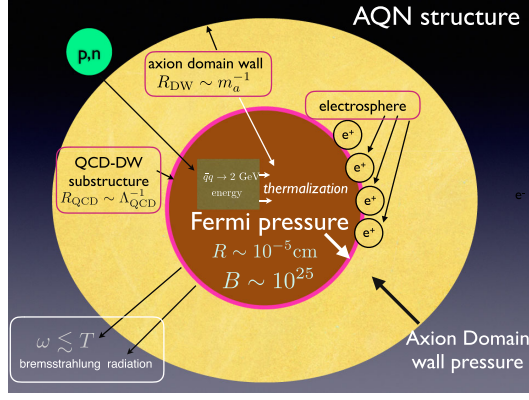
FIG. 1.   AQN structure (not in scale) adopted from [37]. The dominant portion of the energy $\sim$2 GeV produced as a result of a single annihilation process inside the antinugget is released in the form of bremsstrahlung radiation with frequencies $\omega \leq T$. See description and notations in the main text.

B. When the AQNs start to interact with dense environment

For our present work, however, the most relevant studies are related to the effects which may occur when the AQNs made of antimatter propagate in the environment with sufficiently large visible matter density $n(r)$ such as density of the solar corona or the NS's atmosphere. In this case the annihilation processes start and a large amount of energy will be injected to surrounding material, which may be manifested in many different ways. What is more important for the present studies is that the same annihilation processes become much more important if the AQN enters the region of highly ionized plasma because the ions are much more likely to interact with the AQNs in comparison with neutral atoms due to the long-ranged Coulomb attraction.

The related computations on the AQN visible matter interaction originally have been carried out in [38] in application to the galactic neutral environment at present time with a typical density of surrounding baryons of order $n_{\text{galaxy}} \sim$ cm^{-3} in the galaxy. We review these computations with a few additional elements which must be implemented in case of propagation of the AQN in a denser and ionized environment such as the NS's atmosphere.

When the AQN enters the region of the baryon density n the annihilation processes start and the internal temperature increases. A typical internal temperature T of the AQNs can be estimated from the condition that the radiative output must balance the flux of energy onto the nugget

$$F_{\text{tot}}(T)(4\pi R^2) \approx \kappa \cdot (\pi R_{\text{eff}}^2) \cdot (2 \text{ GeV}) \cdot n \cdot v_{\text{AQN}}, \quad (7)$$

where n represents the baryon number density of the surrounding material, and $F_{\text{tot}}(T)$ is total surface emissivity; see below. The left-hand side accounts for the total energy radiation from the AQN's surface per unit time

while the right-hand side accounts for the rate of annihilation events when each successful annihilation event of a single baryon charge produces $\sim 2m_p c^2 \approx 2$ GeV energy. If the environment is represented by neutral atoms and molecules the interaction of the AQNs with environment can be approximated by the geometrical cross section πR^2 for a macroscopically large object of size R. However, if the surrounding material is highly ionized the effective cross section πR_{eff}^2 could be dramatically larger than the geometric value πR^2 due to the long-range Coulomb interaction as the AQN assumes a large negative charge at sufficiently high temperature T; see below for estimates. The factor κ in (7) accounts for large theoretical uncertainties related to the annihilation processes of the (antimatter) AQN colliding with surrounding material.

The total surface emissivity due to bremsstrahlung radiation from the electrosphere at temperature T has been computed in [38] and is given by

$$F_{\text{tot}} \approx \frac{16}{3} \frac{T^4 \alpha^{5/2}}{\pi} \sqrt[4]{\frac{T}{m}}, \quad (8)$$

where $\alpha \approx 1/137$ is the fine structure constant, $m = 511$ keV is the mass of electron, and T is the internal temperature of the AQN. One should emphasize that the emission from the electrosphere is not thermal, and the spectrum is dramatically different from blackbody radiation.

From (7) and (8) one can estimate a typical internal nugget's temperature for the neutral environment when $R_{\text{eff}} \approx R$ and the density n assumes a typical galactic value $n \sim$ cm^{-3}:

$$T \sim 0.4 \text{ eV} \cdot \left(\frac{n}{\text{cm}^{-3}}\right)^{\frac{4}{17}} \cdot \left(\frac{v_{\text{AQN}}}{10^{-3} \text{ c}}\right)^{\frac{4}{17}} \cdot \kappa^{\frac{4}{17}}. \quad (9)$$

Another feature which is relevant for our present studies is the ionization properties of the AQN itself (along with ionization of the surrounding plasma). Ionization, as usual, occurs in a system as a result of the high internal temperature T, in which case a large number of weakly bound positrons from the electrosphere get excited and can easily leave the system. As a result, the antinugget assumes a negative electric charge. Its absolute value $Q(T)$ strongly depends on the environment (density and the temperature).

Precisely this feature of ionization of the AQN dramatically enhances the visible DM interaction in a highly ionized sufficiently dense environment when the cosmologically relevant ratio (σ/M) from (1) could become very large. This feature may dramatically modify many previously obtained results [1–15] which were made under the assumption that DM particles are fundamental weakly interacting objects such as WIMPs.

The emergence of very strong interaction of DM with surrounding material at the star's surface is a direct manifestation of the AQN construction when the dark

matter in the form of the AQNs behaves as *chameleonlike* composite objects. Indeed, the AQNs are the perfect DM particles in a dilute environment as reviewed in Sec. III A but become very strongly interacting objects in a relatively dense environment.

Finally, one should mention here that the AQN model with the same set of parameters to be used in the present work may explain a number of puzzling and mysterious observations which cannot be explained by conventional astrophysical phenomena. These mysterious puzzles occur at many different scales in dramatically different environments, including BBN epoch, dark ages, as well as galactic, Solar and Earth environments at present time; see concluding Sec. IX B.

IV. LESSONS FROM THE SOLAR CORONA HEATING PUZZLE

Before we consider the dynamics of the AQN-NS interaction in Sec. V we would like to make a short detour in this section to overview the application of the AQN framework to the solar corona heating problem [39–42]. The basic lesson from the studies [39–42] is that the energy which heats the corona may come from the annihilation processes of the DM particles in the form of the AQNs in the solar corona. Furthermore, the same AQNs may play the role of *triggers* which may ignite the large solar flares. In other words, the AQNs entering the solar corona may activate the magnetic reconnection in active regions of the sun and initiate the large solar flares.

We shall use the corresponding lessons from [39–42] for the case when AQNs hit the NS, which is the topic of the present studies. Precisely this analogy between the AQN dynamics in a NS's atmosphere versus the solar corona will be our guiding principle in our studies of the AQN-NS interactions in Secs. V–VII.

A. Solar corona heating puzzle: The observations

We start with a few historical remarks. The solar corona is a very peculiar environment. Starting at an altitude of 1000 km above the photosphere, the highly ionized iron lines show that the plasma temperature exceeds a few 10^6 K. The total energy radiated away by the corona is of the order of $L_{corona} \sim 10^{27}$ erg s^{-1}, which is about 10^{-6}–10^{-7} of the total energy radiated by the photosphere. Most of this energy is radiated at the extreme ultraviolet (EUV) and soft x-ray wavelengths. There is a very sharp transition region, located in the upper chromosphere, where the temperature suddenly jumps from a few thousand degrees to 10^6 K. This transition layer is relatively thin, 200 km at most. This transition happens uniformly over the Sun, even in the quiet Sun, where the magnetic field is small (~ 1 G), away from active spots and coronal holes. The reason for this uniform heating of the corona remains to be a mystery.

A possible solution to the heating problem in the quiet Sun corona was proposed in 1983 by Parker [43], who postulated that a continuous and uniform sequence of miniature flares, which he called "nanoflares," could happen in the corona.

The term nanoflare has been used in a series of papers by Benz and coauthors [44–48], and many others, to advocate the idea that these small "microevents" might be responsible for the heating of the quiet solar corona. In most recent studies for the purpose of the modeling the term nanoflare describes a generic event for any impulsive energy release on a small scale, without specifying its cause and its physics nature; see review papers [49,50] with references on recent activities in the field. The list below shows the most important constraints on nanoflares from the observations of the EUV iron lines with SoHO/EIT:

(1) The EUV emission is highly isotropic [45,47]; therefore, the nanoflares have to be distributed very "uniformly in quiet regions," in contrast with flares which have a highly nonisotropic spatial distribution because they are associated with small active regions.

(2) According to [46], in order to reproduce the measured EUV excess, the observed range of nanoflares needs to be extrapolated from the observed events interpolating between $(3.1 \times 10^{24}$–$1.3 \times 10^{26})$ erg to subresolution events with much smaller energies, see item 3 below.

(3) In order to reproduce the measured radiation loss, the observed range of nanoflares needs to be extrapolated to energies as low as 10^{22} erg and in some models, even to 10^{20} erg (see Table 1 in [46]).

(4) The flares, in contrast with nanoflares, originate at sunspot areas, with locally large magnetic fields $\mathcal{B} \sim (10^2$–$10^3)$ G, while the EUV emission (which is observed even in very quiet regions where $\mathcal{B} \sim 1$ G) is isotropic and covers the entire solar surface.

(5) The temporal evolution of flares and nanoflares also appears different. The typical ratio between the maximum and minimum EUV irradiance during the solar cycle does not exceed a factor of 3 between its maximum in 2000 and its minimum in 2009 (see Fig. 1 from [51]), while the same ratio for flares and sunspots is much larger, of the order of 10^2. If the magnetic reconnection (as Parker originally conjectured) was fully responsible for both the flares and nanoflares, then the variation during the solar cycles should be similar for these two phenomena. It is not what is observed: the modest variation of the EUV with the solar cycles in comparison to the flare fluctuations suggests that the EUV radiation does not directly follow the magnetic field activity, and that the EUV fluctuation is a secondary, not a primary effect of the magnetic activity.

B. The nanoflares as the AQN annihilation events

All of the puzzles (such as isotropic features of the EUV emission over the entire solar surface with very modest variations during the solar cycles) as mentioned above can be naturally understood if the EUV emission from the solar corona is related to the DM particles. The corresponding conjecture that the nanoflares heating the corona can be identified with AQN annihilation events[3] has been explicitly formulated in [39]. The main argument supporting this conjecture is an amazing numerical coincidence between the observed total luminosity ($\sim 10^{27}$ erg $\cdot$ s^{-1}) radiated from the corona in the form of soft x rays and EUV and the injected energy resulting from the annihilation events when the AQNs hit the Sun.

Indeed, the impact parameter for capture of the nuggets by the Sun can be estimated as

$$b_{\mathrm{cap}}^{\odot} \simeq R_{\odot}\sqrt{1 + \gamma_{\odot}}, \qquad \gamma_{\odot} \equiv \frac{2\,GM_{\odot}}{R_{\odot}v^2}, \qquad (10)$$

where $v \simeq 10^{-3}$ c is a typical velocity of the nuggets. Assuming that $\rho_{\mathrm{DM}} \sim 0.3$ GeV cm^{-3} and using the capture impact parameter (10), one can estimate the total energy being injected due to the complete annihilation of the nuggets in the solar corona as follows:

$$L_{\odot}^{\mathrm{AQN}} \sim (\pi b_{\mathrm{cap}}^2) \cdot v \cdot \rho_{\mathrm{DM}} \simeq 10^{30}\,\frac{\mathrm{GeV}}{\mathrm{s}} \simeq 10^{27}\,\frac{\mathrm{erg}}{\mathrm{s}}, \qquad (11)$$

where we substitute constant $v \simeq 10^{-3}$ c for numerical estimate.[4] Precisely this "accidental numerical coincidence" between the observed luminosity $L_{\mathrm{corona}} \sim 10^{27}$ erg s^{-1} and the AQN-induced luminosity (11) was the main motivation to put forward the idea that the AQNs represent a new source of energy feeding the EUV radiation from the solar corona, which is very hard to explain in terms of conventional astrophysical sources as highlighted above in Sec. IV A; see also footnote 3 for a comment.

Based on this amazing numerical coincidence the nanoflares have been identified with the AQN annihilation events (within the AQN framework). An immediate self-consistency check of this conjecture is that the lower limit for the AQN baryonic charge (see Table I) approximately

coincides with nanoflare's low energy. Indeed, according to this identification the AQN annihilation of baryon charge B produces the energy $W \simeq 2m_p c^2 B$. One can check that the smallest AQN baryonic charge $B \sim 10^{24}$ as given in Table I is indeed close to the lowest nanoflare's energy $W \sim 10^{21}$ erg. We emphasize that this numerical similarity represents a highly nontrivial self-consistency check of proposal [39], as the acceptable range for the AQNs and nanoflares have been constrained from dramatically different physical systems.

Encouraged by this self-consistency check and the highly nontrivial energetic consideration, a full scale of the Monte Carlo (MC) simulations had been performed in [41]. It has been shown that the annihilation mostly occurs at altitudes around 2000 km where most of the injected energy is released. This represents a highly nontrivial explanation of the emergence of a very narrow transition region of order 200 km width within the AQN framework.

Here we summarize the proposal on identification of the AQN annihilation events with nanoflares: the uniformity of the EUV emission is naturally understood in the AQN framework as DM is distributed very uniformly over the Sun, making no distinction between quiet and active regions. Furthermore, our proposal explains an insignificant role of the magnetic field for the EUV radiation as the AQN events do not depend on the strength of the magnetic field, which is also consistent with observations. It should be contrasted with original conjecture [43] where nanoflares are thought to be scaled down configurations of their larger cousins, which are known to be localized exclusively in the area with large magnetic field, and fed by the magnetic field energy.

Finally, the temporal modulation of the EUV irradiance over a solar cycle is very modest, as opposed to the very dramatic changes in flare activity on the level of 10^2 over the same timescale. This is perfectly consistent with our interpretation of nanoflares being associated with AQN annihilation events which are not related to the solar activity, nor to dynamics of the magnetic field itself during the cycles.

C. AQNs as the triggers of large solar flares

In this section we overview the basic results from [40] where it was argued that the same AQNs (which are identified with nanoflares as overviewed in Sec. IV B) could serve as the *triggers* for large solar flares. The basic reason for necessity for a trigger (which can initiate the magnetic reconnection) to be present in the system is related to very large numerical values of the so-called Lundquist number $S \sim (10^{12} – 10^{14})$ in the solar corona. Precisely this parameter S determines the theoretical value for reconnection time which is much longer than observations show; see the Appendix in [52] for details and references. Although in the last 10–15 years many new ideas have been pushed forward to speed up the

---

[3]In this sense our proposal fulfills a key missing ingredient on the nature of the nanoflares as conventional scaling arguments suggest that the typical timescales for the magnetic reconnection in the background of a typical magnetic field (~ 1 G), must be very long, dramatically longer than the observations suggest; see the Appendix in [52] for details.

[4]A more proper estimation should include $n_{\mathrm{AQN}}(2m_p \cdot B \cdot 3/5)$ where coefficient $3/5$ reflects the portion of the antinuggets, $n_{\mathrm{AQN}} \approx \rho_{\mathrm{DM}}/M_N$ is the density of the AQNs, while $M_N \approx m_p B$ is their typical mass. We ignore all these numerical coefficients in estimate (11) in front of ρ_{DM}.

reconnection, a large number of fundamental questions remains.[5]

The basic idea of [40] is as follows:

(1) The AQNs entering the solar corona with typical velocity of the nuggets $v \sim (600–800)$ km/s in the vicinity of the surface will inevitably generate shock waves as the typical velocities v of the dark matter particles much larger than the speed of sound c_s such that the Mach number $M \equiv v/c_s > 1$, see estimates below.

(2) When the AQNs (distributed uniformly) enter regions with a strong magnetic field in *active regions*, they trigger magnetic reconnection of *preexisted* magnetic configurations.

(3) Technically, the AQNs are capable of sparking magnetic reconnections due to the large discontinuities of the pressure $\Delta p/p \sim M^2$ and temperature $\Delta T/T \sim M^2$ when the AQN-induced shock front passes through the magnetic reconnection regions; see estimates for these parameters below.

Now we estimate the relevant parameters suggesting that the AQNs indeed could serve as the triggers igniting and initiating the large solar flares.

We start our estimate with the speed of sound c_s in the corona at $T \simeq 10^6$ K,

$$\left(\frac{c_s}{c}\right)^2 \simeq \frac{3T \cdot \Gamma}{m_p c^2}, \qquad c_s \simeq 7 \times 10^{-4} \, c \cdot \sqrt{\frac{T}{10^6 \, \text{K}}}, \quad (12)$$

where $\Gamma = 5/3$ is a specific heat ratio, c is the speed of light, and we approximate the mass density ρ_p of plasma by the proton's number density n as follows $\rho_p \simeq n m_p$. The crucial observation here is that the Mach number M is always much larger than one for typical dark matter velocities at the surface:

$$M \equiv \frac{v}{c_s} \simeq 4\sqrt{\frac{10^6 \, \text{K}}{T}} > 1. \quad (13)$$

As a result, a strong shock wave will be generated when the AQNs enter the solar corona. In the limit when the thickness of the shock wave can be ignored, the corresponding formulas for the discontinuities of the pressure p, temperature T, and the density ρ_p are well known and given by (see e.g. [53])

---

[5]One of the questions is the observation of the dramatic variation of timescales when preflare x-ray radiation lasts for seconds, the flare itself lasts for about an hour, while the preparation phase of the magnetic configurations to be reconnected could last for months. The presence of a trigger may automatically resolve this and many other hard questions; see [40].

$$\frac{\rho_{p2}}{\rho_{p1}} \simeq \frac{(\Gamma + 1)}{(\Gamma - 1)}, \qquad \frac{p_2}{p_1} \simeq M^2 \cdot \frac{2\Gamma}{(\Gamma + 1)}$$

$$\frac{T_2}{T_1} \simeq M^2 \cdot \frac{2\Gamma(\Gamma - 1)}{(\Gamma + 1)^2}, \quad M \gg 1, \quad (14)$$

where we assume $M \gg 1$ and keep the leading terms only in the corresponding formulas.

Another important parameter which determines importance of magnetic pressure in comparison with kinetic pressure is dimensionless parameter β:

$$\beta \equiv \frac{8\pi p}{\mathcal{B}^2} \sim 0.05 \left(\frac{n}{10^{10} \, \text{cm}^{-3}}\right)\left(\frac{T}{10^6 \, \text{K}}\right)\left(\frac{100 \, \text{G}}{\mathcal{B}}\right)^2, \quad (15)$$

where for numerical estimates we use typical parameters for the active regions in the corona when $\beta \ll 1$. The same relation (15) also explicitly shows that the magnetic field cannot play any essential role (including a very unlikely possibility of magnetic reconnection) outside the active regions when typical values are $\mathcal{B} \sim 1$ G and $\beta \gg 1$, which was the topic of the EUV radiation in previous Secs. IV A and IV B.

The main assumption for the estimates presented above is that the AQNs can be treated as macroscopically large objects such that conventional classical hydrodynamics applies. In other words, the size of the objects must be much larger than the average distance a between the particles in the surrounding plasma, which itself is determined by the density $a \approx n^{-1/3}$. This condition is perfectly satisfied for the AQNs because their effective size $R_{\text{eff}} \gg 1$ cm is indeed much larger than the geometric size of the quark nugget $R \sim 10^{-5}$ cm due to very strong interaction with surrounding ionized plasma when positively charged ions are captured by the negatively charged nugget; see [41] for the estimate of parameter R_{eff} which indeed satisfies $R_{\text{eff}} \gg a$ for typical density in the corona.

The idea that the shock waves may dramatically increase the rate of magnetic reconnection is not new, and has been discussed previously in the literature, though in a quite different context; see references in the Appendix in [52]. The new element which was advocated in [40] is that the small shock waves resulting from entering AQNs are widespread and generic events in the solar corona. These small events identified with nanoflares and the corresponding annihilation energy is sufficient to heat the corona as estimated by (11). However, they do not generate large flares as $\beta \gg 1$ in quiet regions.

The situation becomes very different however if the nuggets hit the active regions with strong magnetic field $\mathcal{B} \sim 10^2$ G and $\beta \ll 1$. In this case the AQN-induced shock waves may ignite large flare. This proposal may answer many questions of the complicated dynamics of the flares, including a dramatic variation of the timescales as mentioned in footnote 8.

D. Energetics of large solar flares

Now we want to estimate the size and the energy scales associated with such events. We consider separately two different stages. First, we estimate the scales related to the initial phase of the evolution when the AQNs produce the shock waves, but the magnetic reconnection has not started yet. The estimation for the second phase assumes that the magnetic reconnection, leading to a large solar flare, is already fully developed.

In the first, initial stage of the evolution, the magnetic reconnection has not started yet, and the entire energy is related to the shock wave, which itself forms as a result of AQN entering the solar atmosphere from the outer space. In this case a typical timescale when AQN completely annihilates its baryon charge is of order of $\tau \sim 10$ sec; see [39,41]. A typical length scale is determined by the initial velocity of the AQN which is of order $v_{AQN} \sim$ (600–700) km/s such that $L \sim v_{AQN} \cdot \tau \sim 5 \times 10^3$ km. At the same time, a typical radius R of the cone formed by the shock wave is determined by the speed of sound c_s, such that $R \sim M^{-1}L$, where Mach number M is estimated in (13). For numerical estimates below we take $M \simeq 10$. The affected area A due to the shock wave (where the magnetic reconnection starts) is estimated as $A \sim M^{-1}L^2$. We summarize the parameters of the initial stage as follows:

$$\tau \approx 10 \text{ sec}, \qquad L \approx v_{AQN} \cdot \tau \approx 5 \times 10^3 \text{ km},$$
$$R \approx M^{-1}L \approx 10^{-1}L, \qquad A \approx R \cdot L \sim 10^{-1}L^2. \quad (16)$$

We are now in position to estimate the typical energetic characteristics of the system during this *initial* stage. The key element is the observation that the temperature T experiences a large discontinuity resulting from the shock according to (14). Therefore, we estimate a typical internal temperature of the nugget T_2 as follows:

$$\frac{T_2}{T_1} \approx M^2 \approx 10^2, \qquad T_2 \approx M^2 T_1 \approx 10^8 \text{ K}, \quad (17)$$

where $T_1 \sim 10^6$ K corresponds to unperturbed temperature of the solar corona before the shock passage through the area.

An important comment here is that formula (17) shows that the AQN's internal temperature could reach very high values on the level $T \sim 10^8$ K. As a result, the AQNs could be the source of the (1–10) keV x rays. Interestingly enough, the x rays' emission had indeed been recorded for many large flares a few moments (precursor) before the flare starts [54]. Furthermore, one can explicitly see that preflare enhancement propagates from higher levels of the corona into the lower corona and chromosphere [54]. It is difficult to explain such x rays' emission pattern within conventional magnetic hydrodynamics (MHD). In our framework the x ray's emission before the large flare starts is a natural consequence of the proposal when the AQNs (moving from the outer space to the surface) generate the shock and play the role of the triggers initiating and igniting large flares. We further comment on similarity of the x ray's emission from the solar corona during the flare and from the NS in Sec. VIII.

The *second stage* of the flare (after the *initial stage* described above ends) in this framework is represented by the magnetic reconnection ignited by the shock wave. We have nothing new to say about this conventional phase of the evolution. We present the corresponding estimate below for the total flare's energy for completeness and following discussions,

$$W_{flare} \sim \frac{\mathcal{B}^2 V_{flare}}{8\pi} \sim 3 \times 10^{30} \left(\frac{\mathcal{B}}{300 \text{ G}}\right)^2 \left(\frac{V_{flare}}{10^{13} \text{ km}^3}\right) \text{ erg},$$
$$(18)$$

where $V_{flare} \approx L_\perp^2 L$ with $L \sim 5 \times 10^3$ km being a typical length scale (16) where shock waves develop in the solar corona,[6] while $L_\perp^2$ is the area within active region (sunspots) which eventually becomes a part of the magnetic reconnection producing the large flares. Numerically $L_\perp \sim (10^3$–$10^4)$ km for microflares, and it could be as large as $L_\perp \sim 10^5$ km for large flares. It is assumed that precisely this region of volume $V_{flare} = L_\perp^2 L$ with large average magnetic field $\mathcal{B} \sim 300$ G feeds the solar flare as a result of magnetic reconnection. It is also known that the magnetic reconnection is always accompanied by the presence of nontrivial topological structures which manifest a variety of complex processes during the flare; see [40] for references.

It is quite obvious that the energy (18) of a fully developed flare is many orders of magnitude larger than the initial energy of the AQN which serves as a trigger of a large flare. Nevertheless, this initial stage in the flare evolution plays a key role in future development of the system because it provides a very strong impulse with $\Delta T/T \gg 1$ and $\Delta p/p \gg 1$ in a very small and very localized area for a very short period of time (16) in the region where the magnetic reconnection eventually develops. Precisely the presence of a trigger explains a large number of puzzles related to dramatically different timescales which are known to exist in the system; see [40] for references.

We conclude this section on the solar corona heating puzzle with the following remark. Our main topic of this work is the analysis of possible effects which may occur when the AQNs hit a NS's surface. We shall use many lessons from the present section as the magnetic reconnection in a NS triggered and initiated by AQNs may generate many profound effects as we will discuss in the next section.

---

[6]To simplify the estimates we assume the nugget trajectory is perpendicular to the solar surface such that L is oriented along the z direction.

V. WHEN AQN HITS THE NS

A. Energy injection due to the AQN's annihilation

First of all, we would like to estimate a total power being injected as a result of AQN hitting the NS's surface and get annihilated along its path close to the surface. For simplicity we ignore the DM velocity distribution and assume that $v_\infty \simeq 10^{-3}$ c is a typical velocity of the nuggets at a large distance from the NS. In this case the impact parameter for capture and consequent annihilation of the AQNs by the NS can be estimated as follows:

$$\frac{b_{\text{cap}}^{\text{NS}}}{R_{\text{NS}}} \simeq \frac{c}{v_\infty} \cdot \left(\frac{10^6 \text{ cm}}{R_{\text{NS}}}\right)^{1/2} \cdot \left(\frac{M_{\text{NS}}}{2M_\odot}\right)^{1/2} \quad (19)$$

which replaces formula (10) estimated for the Sun. The total energy being injected due to the complete annihilation of the nuggets in the NS is as follows:

$$L_{\text{NS}}^{\text{AQN}} \sim (\pi b_{\text{cap}}^2) \cdot v_\infty \cdot \rho_{\text{DM}} \simeq 10^{23} \frac{\text{erg}}{\text{s}}, \quad (20)$$

which replaces formula (11) with estimate for the Sun; see also footnote 4 with a comment. The estimate (20) of course gives the same order of magnitude for the AQN model as for any other DM model; see e.g. [10] where only kinetic energy of a DM particle contributes to the heating. It should be contrasted with our case when entire energy due to the annihilation will be released. The numerical difference, however, is a very minor effect as all DM particles on the NS's surface become relativistic objects irrespective of the models. As a result, the difference in equilibration temperatures on the surface does not lead to any qualitative observable effects in comparison with previous analysis. In particular, instead of $T \approx 1750$ K from WIMP type models [10] we would get $T \sim 3000$ K from the AQN model, if all released energy is thermalized.

Now we would like to make few comments on comparison of (20) with analogous estimates for the solar corona (11) where the same annihilation events of the AQNs in the solar atmosphere generate fundamentally new phenomenon representing the resolution of the solar corona heating puzzle within the AQN framework as explained in Secs. IV A and IV B.

The dramatic differences in luminosities (4 orders in magnitude) between (11) and (20) is related to the fact that the impact parameters are very different for these two cases. Indeed, factor 10^4 between (11) and (20) can be understood as the ratio

$$\left(\frac{b_{\text{cap}}^\odot}{b_{\text{cap}}^{\text{NS}}}\right)^2 \sim \left(\frac{10^6 \text{ km}}{10^4 \text{ km}}\right)^2 \sim 10^4. \quad (21)$$

As a result, the luminosity ($\sim 10^{27}$ erg $\cdot$ s^{-1}) radiated from the corona (11), though represents only $\sim 10^{-6}$ fraction of the total luminosity of the Sun, nevertheless produces the profound observable effects in the form of the EUV and x ray's emission from the corona. In contrast, the observation of the emission (20) from the NS is unlikely to be directly observed anytime soon.

Indeed, the value for the surface temperature $T \approx 3 \times 10^3$ K as estimated above is way below the present observational capabilities, and we shall not elaborate on this effect of heating due to the direct AQN annihilations in the NS's atmosphere and the crust in the present work. Precisely this effect (heating of the very old stars due to the direct energy injection by DM particles in form of WIMPs) was the main subject of the analysis in most of previous studies [1–12,15]. This is precisely the main conclusion of Sec. II C that DM accretion cannot play any role in heating of the NS to temperatures in the range $T \sim 10^5$ K as observed. This conclusion was entirely based on canonical assumption within the 40-year-old paradigm that DM is represented by a fundamental field in the form of a microscopical particle such as WIMP.

In contrast, the AQN is a complex macroscopical object, outside of this canonical paradigm. Therefore, it may play another role (as a trigger, see below) along with the effect mentioned above.

This work is focused precisely on another consequence of the AQN framework when the nuggets play the role of the triggers which may ignite and initiate much larger events similar to the flares in the Sun as discussed in Secs. IV C and IV D. This effect is not shared by any other DM models when the DM particles are represented by fundamental local quantum fields, such as WIMPs.

When AQN serves as a trigger of a large event such as a flare in the Sun, the dominant portion of the energy feeding such event is coming from a strong magnetic field of the NS (not from the AQN itself) converting its energy into the radiation in broad frequency bands. If this happens there could be many dramatic observable effects, which precisely represents the topic of the present studies.

B. Mach number and shock waves

The goal of the present section is to argue that the AQNs can serve as the triggers which may initiate the magnetic reconnection similar to our discussions in Secs. IV C and IV D in the context of the solar flare physics. Our arguments are based on estimation of different parameters such as β and the Mach number M for a NS environment.

In what follows it is convenient to parametrize the velocity of an AQN when it enters the NS's atmosphere in terms of the proper η_μ velocity and 4-momentum p_μ defined in the usual way:

$$\eta_\mu = \gamma(c, \vec{v}), \qquad \gamma = \frac{1}{\sqrt{1 - v^2/c^2}}, \qquad p_\mu = M_N \cdot \eta_\mu, \quad (22)$$

where $M_N \simeq m_p B$ is the AQN's rest mass expressed in terms of the proton mass as reviewed in Sec. III A.

The key observation here is that the Mach number $M \gg 1$ is always very large for a typical AQN entering the NS's atmosphere,

$$
\begin{aligned}
M &\equiv \frac{\sqrt{v_\perp^2 + v_\parallel^2}}{c_s} \\
&\simeq 6 \times 10^3 \cdot \left(\frac{10^5 \text{ K}}{T}\right)^{1/2} \cdot \left(\frac{10^6 \text{ cm}}{R_{\text{NS}}}\right)^{1/2} \cdot \left(\frac{M_{\text{NS}}}{2M_\odot}\right)^{1/2}
\end{aligned} \quad (23)
$$

which is much larger than one. The shock wave may initiate a large event similar to solar flares considered in Secs. IV C and IV D.

Another important parameter which determines importance of the magnetic pressure in comparison with kinetic pressure is dimensionless parameter β:

$$
\beta \equiv \frac{8\pi p}{\mathcal{B}^2} \sim 10^{-18} \left(\frac{n}{10^{10} \text{ cm}^{-3}}\right) \left(\frac{T}{10^6 \text{ K}}\right) \left(\frac{10^{10} \text{ G}}{\mathcal{B}}\right)^2, \quad (24)
$$

where for numerical estimates we use typical parameters for a NS. The crucial difference with the solar corona here is that $\beta \ll 1$ is very small everywhere on the NS's surface. It is not the case for the solar corona, where $\beta \ll 1$ only in active regions, while $\beta \gg 1$ in quiet regions of the solar surface. As a result, the solar flares occur only in active regions with $\beta \ll 1$ when magnetic reconnection could in principle take place as discussed in Secs. IV C and IV D, while in the NS the magnetic reconnection could occur everywhere at any given moment, and may occupy the entire NS's surface as condition $\beta \ll 1$ holds everywhere.

One more parameter which characterizes the NS's atmosphere is the electron number density n_e where the AQN-induced shock wave may propagate. The uncompensated charge density of electrons and ions in the NS's atmosphere is not vanishing due to the so-called Goldreich-Julian (GJ) effect when the magnetic field spinning through a very good conductor produces the electric field which separates the charges. To be more precise the GJ number density is proportional to $n_{GJ} \propto \mathbf{\Omega} \cdot \mathcal{B}$. Numerically, it can be estimated as follows (see e.g. [55]):

$$
n_e \approx \frac{2\mathcal{B}}{ecP} \frac{R_{\text{NS}}^3}{r^3} \sim \frac{10^{10}}{\text{cm}^3} \left(\frac{1 \text{ s}}{P}\right) \left(\frac{\mathcal{B}}{10^{10} \text{ G}}\right) \left(\frac{R_{\text{NS}}^3}{r^3}\right), \quad (25)
$$

where P is the pulsar period, and r the distance from the center of the star.

If we assume that magnetic reconnection indeed occurs as a result of the AQN triggering event, what could be the energy injection rate in this case? Is it sufficient to heat the old NS to the high temperatures such as $T \sim (10^5$–$10^6)$ K as observed? The corresponding energy is determined by the energy of the magnetic field as a result of successful

reconnection. This injected energy is dramatically larger in comparison with the energy released due to the direct annihilation events of the AQNs in the NS's atmosphere discussed in Sec. V A. The corresponding estimates will be presented in the next section.

VI. MAGNETIC RECONNECTION AS THE HEATING SOURCE OF NS

We are now prepared to present our order of magnitude estimates to argue that the heat being released as a result of the AQN-induced magnetic reconnection events is sufficient to heat the old NS to high temperature $T \sim 10^5$ K as observed. First, we estimate the total hitting rate $\dot{N}$ of the NS by AQNs. It can be estimated by dividing formulas (4) to M_N, i.e.

$$
\frac{dN}{dt} \approx \pi b_\infty^2 v_\infty \left(\frac{\rho_{\text{DM}}}{M_N}\right) \approx \frac{10}{\text{s}} \left(\frac{10^{25}}{\langle B \rangle}\right) \cdot \left(\frac{M_{\text{NS}}}{2M_\odot}\right), \quad (26)
$$

where ρ_{DM} is the local DM density in the vicinity of the NS and $M_N \approx m_p B$ is the mass of the AQN; see Table I.

Our next task is to estimate the minimal required energy to heat the NS's surface to the temperature $T \approx 10^5$ K. The required energy rate to be injected to heat the NS's surface has been estimated previously in (6) and is given by

$$
L = 4\pi R^2 \sigma T_s^4 \approx 10^{29} \left(\frac{T_s}{10^5 \text{ K}}\right)^4 \frac{\text{erg}}{\text{s}}. \quad (27)
$$

The next task is to estimate the total available magnetic energy above the NS's surface. After that one can estimate the portion of the energy which should be converted to the heat to equalize the radiation loss (27). The total magnetic energy $E_{\text{mag}}^{\text{tot}}(A)$ above the NS's surface can be estimated as follows:

$$
E_{\text{mag}}^{\text{tot}} \simeq \frac{1}{8\pi} \int_{r \geq R_{\text{NS}}} d^3x \mathcal{B}^2 \simeq 10^{36} \text{ erg} \left(\frac{\mathcal{B}_{\text{surf}}}{10^{10} \text{ G}}\right)^2, \quad (28)
$$

where we used a simple dipole formula $\mathcal{B} \simeq \mathcal{B}_{\text{surf}} R_{\text{NS}}^3 r^{-3}$ for the estimate.[7]

To make further progress with our computations we assume that every hit by the AQN of the NS triggers and initiates a shock wave which consequently generates the magnetic reconnection. This assumption is very reasonable as a similar assumption for solar flare gives very reasonable estimates for the rate and strength of solar flares as reviewed in Secs. IV C and IV D. Indeed, in both cases the relevant parameters $M \gg 1$ and $\beta \ll 1$ and the shock

---

[7]One should mention here that the estimate (28) represents in fact a lower bound as the relevant magnetic field could be much stronger than a simple dipole formula would suggest; see also comments in Sec. II B.

waves are very likely to be formed. The difference between the Sun and NS is, of course, that flares in the Sun can be generated in active regions only (which accounts for a very tiny portion of the solar surface), while in the NS the shock wave may develop anywhere on the entire NS's surface.

With this assumption we introduce parameter $\epsilon \ll 1$ which describes a small portion of the total magnetic energy (28) which will be converted to heat after AQN strikes the NS and triggers the shock wave leading to the magnetic reconnection with consequent heating of the surface, i.e. $E_{\text{heat}} \equiv \epsilon E_{\text{mag}}^{\text{tot}}$. The corresponding parameter ϵ is estimated from the following condition:

$$\epsilon E_{\text{mag}}^{\text{tot}} \cdot \frac{dN}{dt} = L \Rightarrow \epsilon \approx \frac{L}{\dot{N} E_{\text{mag}}^{\text{tot}}}, \qquad (29)$$

where parameters $\dot{N}$, and L are given by (26) and (27) correspondingly. Numerically, parameter ϵ can be estimated as follows:

$$\epsilon \equiv \frac{E_{\text{heat}}}{E_{\text{mag}}^{\text{tot}}}, \qquad \epsilon \approx 10^{-8} \left(\frac{T_s}{10^5 \text{ K}}\right)^4 \left(\frac{10^{10} \text{ G}}{\mathcal{B}_{\text{surf}}}\right)^2 \left(\frac{\langle B \rangle}{10^{25}}\right), \qquad (30)$$

which implies that the total magnetic energy is more than sufficient to heat old NS to explain the puzzling observations reviewed in Sec. VI. In fact, only a very tiny portion of the magnetic energy ($\sim 10^{-8}$) needs to be converted to heat at each event of the magnetic reconnection triggered by the AQN. In fact the numerical value for ϵ is expected to be even smaller because the relevant magnetic field is likely to be much stronger than a simple dipole formula would suggest; see footnote 7. In what follows we shall argue that this condition can be indeed naturally satisfied.

At this point one could wonder what went wrong with the old (and naively, very generic) argument from Sec. II, suggesting that the magnetic field cannot play any role in heating of the old NS according to (2). The answer is related to two new elements which were completely missed in the naive estimate (2). First, the magnetic field locally could be much stronger than a simple dipole formula would suggest as we already mentioned in footnote 7. Furthermore, as we argue below in Sec. VII, the energy which is powering the magnetic reconnection is related to the magnetic helicity $\mathcal{H}$; see Appendix A for definition and basic features of the magnetic helicity $\mathcal{H}$. Another novel element is the relevant timescale which enters (26) and which is dramatically different from the timescale entering the naive estimate (2). This portion of the magnetic energy could be quickly restored after every AQN-induced event of reconnection with rate (26). A possible mechanism for such "refill" of the magnetic helicity is discussed in items 10 and 11 in the next section and in Appendix A.

VII. MAGNETIC RECONNECTION IN A NS: BASIC INGREDIENTS

In this section we want to formulate the basic ingredients of the proposal supporting our main result formulated in the previous section. It suggests that the magnetic reconnection triggered by the AQN may indeed heat the old NS. In this sense we suggest an alternative mechanism, which we claim is capable to generate enough energy to heat the old NSs to explain the puzzling observations listed in Sec. II.

First of all, we would like to note that the computation of the parameter ϵ defined by (30) from the first principles is not feasible at this point due to very complicated dynamics of the strongly coupled system AQN-NS. In particular, it includes the evolution of the shock waves, developing of the turbulence, and many other accompanied phenomena when the energy transfer occurs from a body moving with enormous Mach number as estimated by (23).

Nevertheless, there are many systems where the magnetic reconnection is known to occur and is believed to power very energetic events such as solar flares discussed in Secs. IV C and IV D. One can use the corresponding observations to support or refute some of the assumptions on dynamical features of the magnetic reconnection in a NS based on experience with the solar flare events.

Another system where magnetic reconnection is believed to play a crucial role (see e.g. [55]) is the magnetars where the so-called fast radio bursts (FRB) are erupted as a result of the magnetic reconnection, see recent review on the topic [56]. While the idea that FRBs are powered by the magnetic field transferring an enormous energy to the radio emission is commonly accepted in the community, the suggested triggering mechanisms which could initiate the magnetic reconnection dramatically vary: from a crust cracking at the NS's surface to sudden triggers from an external event; see [56] for review.

Our proposal [52] that the DM particles in the form of the AQNs play the role of the triggers for FRBs is exactly from the last category when an external object initiates the FRB. In our case the external object is the AQN. In many respects our present proposal that the AQNs could be the triggers of the magnetic reconnections in an old NS which may heat the NS's surface to explain the puzzling observations, as reviewed in Sec. VI, is very similar to proposal [52] in the context of FRBs.

There are many quantitative differences between these two cases, of course: the magnetars from proposal [52] are much younger, have a much stronger magnetic field, and have a much higher surface temperature than the old NS which is the topic of the present work. However, the basic fundamental concept in these two cases is the same: the AQNs can serve as the triggers to ignite and initiate the magnetic reconnection which may feed the very energetic explosions in both cases.

The two systems mentioned above (flares in the solar corona and FRB in magnetars) will be considered as a

toolbox which allows us to test the main proposal of the present work. Indeed, by comparing one or another assumption from the present proposal with similar (analogous) studies of the flares in the solar corona or FRB in magnetars one can support or refute a corresponding assumption. This is precisely the approach we are advocating in this section.

We present below the basic elements of our proposal, item by item. In many items we explicitly point out some similarities between our present system and previously considered systems—flares in the solar corona and FRB in magnetars. Therefore, our assumptions can be confronted with available observations.

(1) The basic conditions such as $M \gg 1$ and $\beta \ll 1$ are satisfied according to (23) and (24), similar to analysis in active regions in the Sun and FRB.

(2) As a result of these conditions the AQN may serve as the trigger to initiate the magnetic reconnection as the environment in all cases is also very similar. Indeed, the density of highly ionized plasma estimated as (25) is close to the density of the solar corona.

(3) Therefore, we expect a strong shock wave generated by propagating AQN, such that the pressure p and temperature T experience strong discontinuities according to (14). This very strong impulse in a very small and very localized area (determined by the AQN's path) for a very short period of time τ may lead to a successful magnetic reconnection.

(4) A typical timescale τ where the shock wave develops is determined by the velocity v_{AQN} of the AQN in the vicinity of the NS's surface, which is close to c. Therefore,

$$\tau \sim \frac{d}{c} \sim \frac{10 \text{ km}}{c} \sim 0.3 \times 10^{-4} \text{ s}, \qquad (31)$$

where distance $d \sim 10$ km is determined by the region where the density of the ionized gas is sufficiently large (25).

(5) The timescale τ determines the size of the cone where the shock wave develops and where the pressure p and temperature T experience strong discontinuities, similar to the solar flare analysis (17).

(6) This AQN-induced shock will trigger the magnetic reconnection in the area A estimated as

$$A \approx dc_s\tau \approx \frac{d^2}{M} \sim 10^{-4}d^2, \qquad (32)$$

which represents a small portion $\sim(10^{-4}$–$10^{-5})$ of the NS's surface. This area has the same physical meaning as estimate (16) for the solar flare which defines the area for the initial stage of the magnetic reconnection. The difference with the solar flare is that the magnetic reconnection could only occur in a small active region of the Sun where the magnetic field is large and the condition $\beta \ll 1$ is satisfied, while the reconnection in the NS may occur anywhere on the surface as condition $\beta \ll 1$ is satisfied everywhere.

(7) Therefore, if magnetic reconnection starts in one location, it may quickly sweep out (potentially) an entire NS's surface. In this case the total energy of the event in the NS [*second stage* in the classification (18) in the context of solar flares] represents a finite portion of the integral (28). It must be contrasted with the solar flare estimate (18) which represents a very tiny portion of the surface in comparison with the total surface of the Sun (the so-called active regions, the sunspots).

(8) The speed of magnetic reconnection is governed by dimensionless parameter β_{in} in notations [52,55], where "in" in β_{in} stands for inflow speed. It must be sufficiently high for fast successful reconnection, but it must be much slower than the speed of light $\beta_{\mathrm{in}} \ll 1$. If we formulate this condition in terms of the reconnection typical timescale $\tau_{\mathrm{in}} \equiv d \cdot \beta_{\mathrm{in}}^{-1}$ the following hierarchy scales must be satisfied[8]:

$$\tau \ll \tau_{\mathrm{in}} \ll \dot{N}^{-1} \rightarrow 0.3 \times 10^{-4} \text{ s} \ll \tau_{\mathrm{in}} \ll 0.1 \text{ s}, \quad (33)$$

where parameter τ is determined by the AQN serving as a trigger, see (31), while timescale $\dot{N}^{-1}$ is a typical timescale between two independent consecutive events according to (26).

(9) The dynamics of magnetic reconnection studied in the context of FRB suggests that the energy powering FRB is the magnetic helicity $\mathcal{H}$; see Appendix A for the definition and short introduction into the subject. We assume that this feature on the dominant role of the $\mathcal{H}$ holds for the present proposal as well. The basic argument for this assumption is that the environments of NSs and magnetars are very similar.

The magnetic reconnection implies that the electric field $E_{\parallel}$ during the reconnection time τ_{in} will be induced; see [52,55]. Its direction should be parallel to the original static magnetic field $\mathcal{B}$ with the coefficient proportional to β_{in}, i.e.

$$E_{\parallel}(\text{induced}) \propto \beta_{\mathrm{in}}\mathcal{B}. \qquad (34)$$

---

[8]Parameter β_{in} was estimated in [55] in the context of FRB physics. It determines the duration of the magnetic reconnection as $\tau_{\mathrm{FRB}} \propto \beta_{\mathrm{in}}^{-1} \approx 10^{-3}$ s. Parameter τ_{FRB} plays the same role as τ_{in} in (33). A similar parameter (duration of the large flare) in the context of solar physics could be as long as a few hours, while the duration of the initial stage of the flare lasts about 10s, see (16). In all cases the ratio between the duration of the trigger event (due to the AQN) and the magnetic reconnection itself is about $\sim1\%$.

The condition (34) unambiguously implies that very specific electromagnetic (E&M) configuration with $\sim \vec{E} \cdot \vec{\mathcal{B}} \propto \beta_{\text{in}} \mathcal{B}^2$ must be generated during the reconnection. The main feature of this configuration is that it enters the formula (A2) which describes the dissipation of the magnetic helicity $\mathcal{H}$. Precisely the dissipation of the magnetic helicity $\mathcal{H}$ powers the magnetic reconnection. Assuming $\beta_{\text{in}} \sim 1\%$ [which is within the window (33)] one can infer that every event of the magnetic reconnection will convert $\sim 1\%$ of its magnetic helicity into the heat along with other radiation losses such as x rays. Such a relatively high efficiency rate is obviously more than sufficient to generate energy heating the NS's surface according to (30) even if one assumes that only a small finite portion of the surface (rather than the entire NS) will be experiencing the magnetic reconnection.

(10) It is very likely that there are some mechanisms which restore the energy associated with magnetic helicity dissipation (due to the magnetic reconnection) and restore its equilibrium value. Indeed, there are some observations in the FRB context suggesting that frequency of some FRB repeaters is enormously high. For example, rFRB 20121102A emitted a total amount of energy $\sim 3.4 \times 10^{41}$ erg in the radio band from 1652 bursts detected in 59.5 hours in a 47-day time span [56,57]. Assuming that this activity represents a typical behavior of the FRB repeaters, one could infer that there must be a mechanism which restores the magnetic source of the energy.[9]

Based on this observation (in a FRB context) we assume that there should be an operational mechanism which restores the energy reservoir (28) by equilibrating the system after the events of reconnection which heat the NS's surface; see also footnote 7 on numerical value for the relevant value of $\mathcal{B}$ entering formula (28).

(11) A possible mechanism of equilibration which could potentially restore the magnetic energy had been discussed previously in a very different context in [58]. Important conclusion of these studies was that the magnetic helicity $\mathcal{H}$ which is powering the magnetic reconnection (see item 9) is a very generic feature of the NS, and in fact there are many observational evidences suggesting that the magnetic helicity $\mathcal{H}$ must be present in the NS. We

overview the basic results of these studies below and refer the reader for details to Appendix A.

(12) The basic argument presented in [58] is that the so-called topological nondissipating currents will be induced in the NS as a result of quantum anomalies in high density QCD. These currents might be responsible for many observed phenomena such as a NS's kicks, toroidal magnetic field, and the magnetic helicity, to name just a few. This is a very generic and well-known phenomenon in QCD. It is related to the asymmetry between left-handed and right-handed chemical potentials which could be generated by $\mathcal{P}$-odd weak interactions. Formally, it could be expressed as generation of the so-called axial chemical potential $\mu_5 \equiv 1/2(\mu_R - \mu_L)$.

The $\mu_5 \neq 0$ in context of the heavy ion physics in QCD leads to a number of $\mathcal{P}$ odd effects, such as chiral magnetic effect, chiral vortical effect, and charge separation effect, to name just a few. This field of research initiated in [59] became a hot topic in recent years as a result of many interesting theoretical and experimental advances; see recent review papers [60,61] on the subject.

In the context of the present work of NS physics, one should mention that there is strong observational evidence, see e.g. [62] and references therein, supporting the presence of the toroidal magnetic field which unambiguously suggests that the magnetic helicity $\mathcal{H}$ must be nonzero in neutron stars. We consider this as an indirect observational evidence supporting the claim that $\mathcal{P}$-odd topological currents [58] had been induced at some early moment in the star's evolution.

(13) If one assumes that the magnetic helicity $\mathcal{H}$ is present in the system at the moment of magnetic reconnection, it is expected from (34) that the energy feeding the magnetic reconnection comes from the magnetic helicity $\mathcal{H}$, which is directly related to the toroidal magnetic field in the system; see Appendix A for additional comments. One should emphasize that the toroidal magnetic field is generated by nondissipating topological current (A7), in contrast with a typical dipole type field (28) which is generated by usual dissipating currents satisfying the conventional Ohm's law (A6) in the core of the NS.

(14) In order to understand what happens when the magnetic reconnection event occurs, one should recall that the NS's system (which includes the dipole type magnetic field, the toroidal magnetic field, the magnetic helicity $\mathcal{H}$, and the nondissipating topological current with many other conventional components) is a very complicated dynamical self-interacting and self-equilibrating system. It implies that if some elements of the system suddenly get changed, the other elements of the system will adjust their values to restore the equilibrium of the system.

---

[9]The total energy emitted would exceed 6.4×10^{45} erg assuming a radio efficiency 10^{-4}, which we consider is already too high. This is a substantial fraction of the available magnetic energy from a magnetar [56]. This estimate again strongly suggests that there must be a mechanism restoring the magnetic energy after the eruptions as example of the rFRB 20121102A already pose significant energy budget issues [56].

In context of the reconnection events it implies that the removing (due to reconnection) some value of the magnetic helicity $\mathcal{H}$ will result in modification of the currents and chemical potential μ_5 to restore its equilibrium values. This equilibration is formally expressed by (A5).

The reservoir of the chemical potential μ_5 is truly enormous as estimate (A11) suggests. Therefore, we propose that the mechanism of equilibrating the magnetic helicity $\mathcal{H}$ as suggested above, in principle, is capable of restoring the energy associated with magnetic helicity after the events of reconnection; see Appendix A with additional comments and clarifications.

We conclude this section with the following comment. All analytical expressions as presented above should be taken very cautiously as they had been derived from comparison with a different system with dramatically different parameters. Nevertheless, the basic fundamental principles (the magnetic reconnection triggered by an external object) are very much the same. As a result we expect that our estimates give a qualitatively correct big picture. The magnetic reconnection, its evolution, and the triggering mechanisms are obviously the prerogative of numerical simulations which can support or refute the hypothesis advocated in this work. Therefore, we strongly advocate the researchers in relevant fields to consider this picture seriously. A hope is that the recent advancements in the field can successfully attack these complicated technical problems and test the heating mechanism as advocated in this proposal.

Another option to test this proposal (which is complimentary to numerical tests mentioned above) is to measure some specific observables which always accompany the magnetic reconnection. This is the topic for the next section.

VIII. X RAYS AS THE INDICATORS OF THE MAGNETIC RECONNECTION IN NSs

First, we start by mentioning that it has been known for quite some time that the solar flares are normally accompanied by strong x-ray radiation, see e.g. [54] for a review of the last complete solar cycle No -24. Furthermore, the x rays are considered to be a good indicator for large flares because the x ray's intensity dramatically increases few moments before a flare starts.

In addition to that, it has been pointed out in [54] that the solar preflare enhancement in the form of the x rays propagates from higher levels of the corona into a lower corona and chromosphere; see Fig. 8 in [54]. This preflare enhancement is a very puzzling and unexpected phenomenon as preflare propagates from top to bottom. Nevertheless, these unusual temporal and spatial patterns of propagation have a very natural explanation within the AQN framework (reviewed in Sec. IV D in the context of solar flares) because the AQNs propagate (and ignite the magnetic reconnection) from the outer space to the surface.

Now we return to our main topic of the NS. The leitmotif of the proposal advocated in this work is that of two naively very different phenomena (in dramatically different systems):

(1) the heating mechanism of relatively old NS, and
(2) the solar flares

are in fact very similar as they are both powered by the same mechanism of the magnetic reconnection (according to the proposal) triggered and initiated by the dark matter AQN particles. Therefore, we expect that a number of accompanying effects associated with magnetic reconnections must also manifest themselves in very similar ways in both cases. One such profound accompanying effect of large solar flares is the x ray's emission; see first paragraph of this section. Therefore, we expect that a similar x-ray emission must be also present in the NS if the NS's heating is indeed powered by magnetic reconnection as advocated in this work.

The main goal of this section is to estimate the x-ray's intensity from the NS by using (for normalization) the observed and well-recorded intensity of the x ray's radiation during the solar flares. In this estimate we use the same logical steps as in Secs. V–VII by comparing one and the same phenomenon in two different systems.

A. X rays from solar flare as normalization point

The starting point of our estimates is as follows. The peak of the x rays in the band 0.1–0.8 nm of the flare of 9 August 2011 is recorded as follows (see Fig. 8 in Ref. [54]):

$$
F_X^\odot \approx 10^{-3} \; \frac{\mathrm{W}}{\mathrm{m}^2} \approx \frac{\mathrm{erg}}{\mathrm{s} \cdot \mathrm{cm}^2},
$$
$$
E \in (1.5\text{–}12.4) \; \mathrm{keV}, \tag{35}
$$

while the average $\langle F_X^\odot \rangle$ of the x ray's emission during the flare can be estimated as $\langle F_X^\odot \rangle \approx 10^{-2} \; \mathrm{erg} \cdot \mathrm{s}^{-1} \cdot \mathrm{cm}^{-2}$ which is almost 2 orders of magnitude smaller than the peak value (35). At the same time the total flux from the flare emitted from all frequency bands can be estimated as

$$
F_{\mathrm{tot}}^\odot \approx 10 \left(\frac{E_{\mathrm{tot}}}{10^{32} \; \mathrm{erg}} \right) \; \frac{\mathrm{erg}}{\mathrm{s} \cdot \mathrm{cm}^2},
$$
$$
\xi \equiv \frac{\langle F_X^\odot \rangle}{F_{\mathrm{tot}}^\odot} \approx (10^{-2}\text{–}10^{-3}) \tag{36}
$$

assuming that the flare lasts about 1 h and the total released energy E_{tot} during a large flare was between 10^{31} erg and 10^{32} erg. The order of magnitude estimate (36) suggests that the x-ray's flux represents less than a 1% portion of a large flare. We use this ratio ξ to estimate the x-ray's flux from the NS due to the magnetic reconnection in the next subsection.

B. X rays from NSs originated from magnetic reconnection

In our estimates which follow, we assume that the observed temperatures of sufficiently old NSs are entirely saturated by the magnetic reconnection mechanism as advocated in this work. This is obviously a strong assumption. However, as reviewed in Sec. II, any common mechanisms such as rotochemical heating cannot explain many observations; see Sec. II A. In particular, the so-called magnificent seven stars cannot be explained by this mechanism with reasonable changes of the parameters; see Fig. 3 in [23]. There are many similar cases when the observed temperature of a NS dramatically exceeds the theoretical estimates and is inconsistent with the canonical picture of cooling, including additional mechanisms reviewed in Sec. II.

With this assumption in mind, and assuming the blackbody radiation spectrum, we estimate the total flux of E&M radiation (powered by magnetic reconnections, as presented in Sec. VII) as follows:

$$F_{\text{tot}}^{\text{NS}} = \frac{L}{4\pi r^2} \sim \frac{7 \times 10^{32}}{4\pi r^2} \left(\frac{T_s}{10^6 \text{ K}}\right)^4 \frac{\text{erg}}{\text{s}}$$

$$\sim 6 \times 10^{-10} \left(\frac{T_s}{10^6 \text{ K}}\right)^4 \left(\frac{0.1 \text{ kpc}}{r}\right)^2 \frac{\text{erg}}{\text{s} \cdot \text{cm}^2}, \quad (37)$$

where r is the distance to the NS, while the luminosity L is estimated in (6).

We need two more elements to complete our estimate for $\langle F_{\text{X}}^{\text{NS}}\rangle$ analogous to $\langle F_{\text{X}}^{\odot}\rangle$ entering (36). First, we assume that the ratio $\xi \sim 10^{-3}$ defined by (36) is the same for the solar flares and NSs because (according to our proposal) two different phenomena are originated from the same physics of the magnetic reconnection as argued above. Another element which is also important for our estimate of $\langle F_{\text{X}}^{\text{NS}}\rangle$ is the ratio of two different timescales: first, the τ_{in} is the reconnection timescale, which represents the duration of the magnetic reconnection, while $\dot{N}^{-1}$ is a typical timescale between two independent consecutive events as defined in (33). As a result, we arrive at the following estimate for the x ray's flux from the NS due to the magnetic reconnection[10]:

---

[10]The timescale τ_{in} enters the formula (38) because x rays can be emitted exclusively during the reconnection period according to our proposal, similar to discussions of the x ray's radiation during the solar flare from Sec. VIII A. At the same time the τ_{in} is normalized by a typical timescale $\dot{N}^{-1}$, which represents a timescale before the next AQN hits the NS when new reconnection starts and new portion of the energy is injected into the NS's atmosphere. We assume that the energy will be eventually thermalized, which justifies our formula for luminosity (37) with the blackbody radiation spectrum.

$$\langle F_{\text{X}}^{\text{NS}}\rangle \sim \xi \cdot \left(\frac{\tau_{\text{in}}}{\dot{N}^{-1}}\right) \cdot F_{\text{tot}}^{\text{NS}} \sim \left(10^{-4}\text{--}10^{-5}\right) F_{\text{tot}}^{\text{NS}}$$

$$\sim \left(10^{-13}\text{--}10^{-14}\right) \left(\frac{T_s}{10^6 \text{ K}}\right)^4 \left(\frac{0.1 \text{ kpc}}{r}\right)^2 \frac{\text{erg}}{\text{s} \cdot \text{cm}^2}, \quad (38)$$

where for the numerical estimate we use $\tau_{\text{in}} \sim 10^{-3}$ s (motivated by the FRB analysis) and $\dot{N}^{-1} \simeq 0.1$ s; see footnote 8 with some comments.

One should emphasize that this is really an order of magnitude estimate—it is very hard to improve it as the estimate (38) includes a large number of elements with unknown physics. Furthermore, many NSs are known to be emitters of x rays due to many other reasons (for example, due to the conversion of the spin-down power into the x rays). Therefore, our estimation (38) should be considered as an additional contribution to the x ray's emission. It obviously implies that it is very hard to discriminate the x ray's emission flux as given by (38) from many other canonical astrophysical mechanisms. However, there are known special cases when conventional astrophysical mechanisms produce a very tiny contribution to the x ray's radiation, in which case (38) could play the dominant role, and in principle could be discriminated from other mechanisms, see example below.

It is instructive to present a numerical value of the flux $\langle F_{\text{X}}^{\text{J1856}}\rangle$ for $J1856$ from magnificent seven (M7) stars which are the closest to Earth. These NSs belong to the category when the star's temperature greatly exceeds an anticipated value as reviewed in Sec. II A. The corresponding flux $\langle F_{\text{X}}^{\text{J1856}}\rangle$ is estimated from (38) as

$$\langle F_{\text{X}}^{\text{J1856}}\rangle \approx \left(4 \times 10^{-15}\text{--}4 \times 10^{-16}\right) \frac{\text{erg}}{\text{s} \cdot \text{cm}^2} \quad [\text{estimation}], \quad (39)$$

where we use $r \approx 0.123$ kpc and $T_s \approx 0.5 \times 10^6$ K for the numerical estimates. It is quite remarkable that the x ray's emission has indeed been observed [63] from this star with 5σ excess in a (2–8) keV energy range with result

$$\langle F_{\text{X}}^{\text{J1856}}\rangle = \left(1.5_{-0.6}^{+0.7}\right) \times 10^{-15} \frac{\text{erg}}{\text{s} \cdot \text{cm}^2} \quad [\text{observations}]. \quad (40)$$

According to [63] it is difficult to explain this excess of x-ray radiation by any conventional astrophysical sources or any systematic effects. This observation nicely falls into the interval (39). We consider this result as a highly nontrivial consistency check for the application of the AQN framework to the NSs heating problem as the parameters entering the estimate (38) are based on dramatically different physics describing enormous ranges of scales in drastically different contexts, from DM distribution to solar

physics. All of the corresponding parameters had been fixed long ago in applications to different systems, without any attempt to modify or fit them to match the present observations. Therefore, (38) could be potentially many orders of magnitude off from the observed value (40).

In many aspects the similarity of the numerical values between (39) and (40) is analogous to the similarity between the observed solar corona luminosity $L_{\text{corona}} \sim 10^{27}$ erg s^{-1} in EUV and the AQN-induced luminosity (11) which is entirely determined by the DM parameters, not related to the solar corona. Therefore, we think it is very hard to interpret the numerical agreement between (39) and (40) as simply an "accidental numerical coincidence." We think it should be interpreted, similar to mysterious solar corona EUV radiation, as a result of some deep roots and connections between DM physics and NSs physics, which is naturally incorporated by the AQN framework.

IX. CONCLUDING COMMENTS AND FUTURE DEVELOPMENTS

The presence of the *antimatter* nuggets in the system implies, as reviewed in Sec. III, that there will be annihilation events (and continuous injection of energy at different frequency bands) leading to a large number of observable effects on different scales: from early Universe to the galactic scales to the Sun and the terrestrial rare events.

In the present work we focus on manifestations of these annihilation events on physics of the NS. We proposed that DM in the form of the AQNs may serve as the triggers igniting the large explosive events powered by the magnetic reconnection. The released energy as a result of these events may serve as the heater of NSs as suggested in Sec. VI. This is precisely the additional source of energy which may resolve the mysterious and puzzling observations as reviewed in Sec. II when the NS's temperature is inconsistent with canonical cooling mechanisms.

One should emphasize once again that a precise measuringof the NS's surface temperature is a very subtle point such that all recorded values should be taken with some scepticism; see footnote 2 with a comment. Nevertheless, we believe that the observed discrepancy between measured and predicted temperatures is a real physical effect, and we propose a specific mechanism which could be responsible for the excess of the heating.

We do not need to repeat the key elements on physics of the magnetic reconnection triggered by the AQNs as presented in Sec. VII in this conclusion. Instead, we want to mention below several phenomena which should accompany the proposed mechanism of the excess of heating of old NSs. As such these additional emissions should be considered as possible tests and predictions for a proposed mechanism of heating.

In Sec. IX A we list some possible new tests which can substantiate or refute our proposal. Finally, in Sec. IX B

we describe several other mysterious and puzzling observations (outside the NS's system), which can be understood within the same AQN framework. We consider this as indirect support for our proposal as the computations are based on the same set of parameters of the AQN model reviewed in Sec. III.

A. Possible tests of the proposal

As mentioned at the very end of Sec. VII there are several tests which can substantiate or refute this proposal on a heating mechanism of the old NSs. One of them is a numerical study of evolution of the magnetic reconnection, its evolution, and the triggering mechanisms which are obviously the prerogative of numerical simulations. Another, complimentary approach (which represents the topic of the present section) is the analysis of the radiation in very broad frequency bands (from radio to hard x rays, and likely to gamma rays) which always accompany the heating mechanism suggested in Secs. VI and VII.

There is an enormous energy reservoir (A11) which could be converted to the magnetic helicity and eventually to the heat and E&M radiation. We specifically focus on hard x-ray radiation in Sec. VIII because we consider this frequency band to be the most promising channel where this heating mechanism can be directly tested. Another possible radiation in the radio frequency bands which also accompanies the magnetic reconnection is expected to be less promising as the estimates in Appendix B imply.

Essentially we suggest to study the hard X ray emission from other M7 stars as estimation (38) applies to all of them. As we mentioned in Sec. II all M7 stars have the temperatures which greatly exceed the expectations. We interpret this inconsistency as the presence of the additional heating mechanism in the form of the magnetic reconnection for all M7 stars in spite of subtleties related to the measured surface temperature as mentioned in footnote 2. Therefore we predict that all M7 stars should emit the hard x rays which always accompany the reconnection with flux being estimated in (38). As mentioned in [63] the observation of the hard x ray from J1856 with 5σ excess (and not observations of a similar signal in other M7 stars) could be related to the fact that J1856 has the most exposure time across all of the x-ray cameras that were considered in [63].

Another possible class of NS where a proposed heating mechanism could manifest itself is represented by very old pulsars. As mentioned in Sec. II the observed temperatures (well exceeding $T_s \gtrsim 10^5$ K) of many old pulsars with $t \gtrsim 10^8$ yr cannot be explained by conventional mechanisms; see review [23] with details. At the same time, there are many cases where such high (and even much higher) surface temperatures have been observed. As an illustrative sample from this class, one could consider PSR J0108-1431 which is a nearby ($r \simeq 0.13$ kpc), 170 Myr old pulsar. Its surface temperature is known to be very high:

$(1–5) \times 10^5$ K and it is hard to explain even with additional heating mechanisms [23].

It is also interesting to note that this pulsar is observed in an x ray with flux $\langle F_X^{J0108} \rangle = (9 \pm 2) \times 10^{-15} \; \frac{\text{erg}}{\text{s}\cdot\text{cm}^2}$ in the (0.3–8) keV band. It is very similar in value to (40) observed in (2–8) keV band, if one excludes the soft x-ray segment from $\langle F_X^{J0108} \rangle$ representing its dominant portion as the corresponding spectrum has a power law with index $\gamma \simeq 2.2$, see [64]. This similarity between two different cases is consistent with our formula (38) as the temperatures and distances for both NSs are almost the same.

One should note that in the original paper [64] the relatively large flux $\langle F_X^{J0108} \rangle$ was entirely attributed to a spin-down mechanism with enormously high x ray efficiency $\eta_X \simeq 0.4 \times 10^{-2}$, while for typical younger pulsars similar x ray efficiency is 2 orders of magnitude smaller: $\eta_X \simeq (10^{-5}–10^{-4})$. In our view it is very hard to justify such dramatic increase of the x ray's efficiency for older pulsars from the theoretical side. We are more inclined to interpret a sufficiently high x-ray flux $\langle F_X^{J0108} \rangle$ as a manifestation of the magnetic reconnection which powers the heating of this old pulsar, and accompanied to this heating the x-ray emission as estimated in Sec. VIII.

Another possible test of the proposed heating mechanism is a study of thermal pattern on the NS's surface. The main observation here is that the magnetic reconnection is powered by magnetic helicity $\mathcal{H}$ (on large and small scales). Consequently, the toroidal magnetic field is expected to play an essential role in the dynamics and heating of the NSs as discussed in Sec. VII. It implies that the thermal pattern on the NS's surface must be very different from a canonical poloidal dipolar magnetic field (in which case the cold region is always localized along the equator while the hot regions are always localized around the poles). These topics are obviously a prerogative of numerical simulations which can support or refute the hypothesis advocated in this work. It can be only accomplished with comprehensive numerical simulations of a magneto-thermal coupled evolution which includes such elements as the magnetic reconnection, its evolution, and the triggering mechanisms.

In addition, an observation of the magnetic field during the solar flares in active regions which always demonstrates very complex topological structure as mentioned in Sec. IV D supports the complex structure of the field as a consequence of this proposal. Therefore, an observation of any correlations between the complex thermal pattern, higher than expected average temperature of a NS, and the excess of the hard x ray could (implicitly) support the proposed heating mechanism. In fact, some recent studies apparently indicate, see review [65] for references, that the thermal patterns of the NSs very often display a complicated structure, dramatically different from a canonical poloidal dipolar magnetic field pattern.

B. Other (indirect) evidences for DM in the form of the AQN

There are many hints (outside the NSs physics which represent the topic of the present work) suggesting that the annihilation events, which are an inevitable feature of this framework, may indeed have taken place in the early Universe as well as in present epoch at very different scales. In particular, in the early Universe the AQNs do not affect BBN production for H and He, but might be responsible for a resolution of the "primordial lithium puzzle" due to its large electric charge $Z = 3$; see [35] for details.

The very same interaction of the visible-DM components may lead to many observable effects during the galaxy formation epoch. Indeed, while the cold dark matter model works very well on large scales, a number of discrepancies have arisen between numerical simulations and observations on subgalactic scales; see e.g. recent review [66] and references on original papers therein. Such discrepancies have stimulated numerous alternative proposals including, e.g. self-interacting dark matter, self-annihilating dark matter, decaying dark matter, and many others; see [66] and erences therein. Our comment here is that the AQN model represents a specific example of a strongly interacting chameleonlike model: the AQNs do not interact with the surrounding material in a dilute environment, but strongly interact with baryonic material in a sufficiently dense environment at the galactic scale, which helps one to resolve many observed discrepancies during the structure formation epoch [67].

The very same interaction of the visible-DM components may lead to a large number of observable effects also at present epoch. In particular, trecent studies [68–70] suggest that there is a strong component of the diffuse far-ultraviolet (FUV) background which is very hard to explain by conventional physics in terms of the dust-scattered starlight. As argued in [71] the mysterious and puzzling observations of the diffuse FUV could be directly related to the annihilation events of the AQNs propagating in the galactic media. There are numerous similar examples in many frequency bands (from radio to optical bands to UV to x rays) when the observations require an additional energy injection into the system. The AQN annihilation events may provide this required (by observations) additional source of radiation.

We conclude this work with the following final comment. We advocate the idea that study of specific features of NSs as mentioned in Sec. IX A could shed some light on the nature of DM. It is a most unexpected turn of our studies as it allows (implicitly) study the nature of DM by analyzing some subtle features of NSs.

The new paradigm on the nature of cold DM (when it is represented in the form of macroscopical large objects as reviewed in Sec. III instead of commonly accepted WIMPs) has many consequences which are mentioned above, and which are consistent with all presently available

cosmological, astrophysical, satellite, and ground-based observations. In fact, it may even shed some light on the long-standing puzzles and mysteries (outside of NSs physics) as mentioned above and in Sec. IV.

APPENDIX A: MAGNETIC HELICITY $\mathcal{H}$ AND ITS ROLE IN MAGNETIC RECONNECTION

The main goal of this appendix is to overview some important results on the magnetic helicity which is a topological invariant, and represents the observable which characterizes the dynamics of the magnetic reconnection. Needless to say, the magnetic reconnection, according to our proposal, plays a crucial role in transforming the static magnetic energy into the flare type events (similar to the solar flares) which could heat the old NSs.

There are several elements which we would like to overview in this appendix. First of all, we would like to explain why magnetic helicity $\mathcal{H}$ plays a key role in reconnection. Secondly, we want to argue that the magnetic energy related to the helicity $\mathcal{H}$ could be potentially restored as a result of coupling the helicity $\mathcal{H}$ with a reservoir of the chirality which could be generated when the NS was sufficiently hot. Finally, we also want to argue that the chirality reservoir is truly enormous in a NS.

We start with a definition[11] of the magnetic helicity in volume V which can be represented as follows [72]:

$$\mathcal{H} \equiv \int_V \vec{\mathcal{A}} \cdot \vec{\mathcal{B}} \, dV, \tag{A1}$$

where $\vec{\mathcal{A}}$ is the vector potential corresponding to the magnetic field $\vec{\mathcal{B}} = \vec{\nabla} \times \vec{\mathcal{A}}$. It is known that the magnetic helicity $\mathcal{H}$ in general is not a gauge invariant observable because the gauge potential $\vec{\mathcal{A}}$ is not a gauge invariant object. However, if one requires that the magnetic field is tangent on the surface boundary ∂V of V, i.e. $\vec{\mathcal{B}} \cdot \vec{n}|_{\partial V} = 0$,

the magnetic helicity becomes a well-defined gauge invariant object, see e.g. [72].

In the simplest case when the magnetic configuration can be represented in the form of two interlinked (but not overlapping) tubes with fluxes Φ_1 and Φ_2, the magnetic helicity $\mathcal{H}$ counts its linking number, i.e. $\mathcal{H} = 2\Phi_1\Phi_2$ is proportional to an integer linking number if fluxes Φ_1 and Φ_2 are quantized. This is precisely the reason why the magnetic helicity is the topological invariant and cannot be easily changed during its evolution. In fact, the crucial property of the magnetic helicity $\mathcal{H}$ is that it is exactly conserved during the time evolution in ideal MHD [72]. It is also known that the magnetic helicity $\mathcal{H}$ is odd under the $\mathcal{P}$ symmetry corresponding to $\vec{x} \to -\vec{x}$ transformations. This implies that the magnetic helicity can be only induced if there are $\mathcal{P}$ violating processes producing a large coherent effect on macroscopic scales. We refer to one of the proposals [58] with specific estimates on how it could happen.

In what follows we also need the expression for the temporal variation of magnetic helicity as it is directly related to the dissipation rate. Differentiating Eq. (A1) one arrives to

$$\frac{d\mathcal{H}}{dt} = -2 \int_V \vec{E} \cdot \vec{\mathcal{B}} \, dV, \tag{A2}$$

where we ignored the surface boundary term, see e.g. [73,74] with explicit derivations. A key observation here is that the dissipation term in (A2) is proportional to $\sim \vec{E} \cdot \vec{\mathcal{B}}$ which is precisely the E&M configuration which emerges as a result of the magnetic reconnection as formula (34) states. As explained in the text the induced electric field parallel to the original static magnetic field is absolutely a required feature for the successful magnetic reconnection. The relation (A2) answers the question of why the magnetic helicity $\mathcal{H}$ is the key player of the reconnection.[12]

There is one more important element here on the relation between the magnetic helicity and the chirality which needs to be explained. In the chiral limit the axial current is not conserved as a result of quantum anomaly, see e.g. review papers [60,61] on the subject, i.e.

$$\partial_\mu J_5^\mu = \frac{e^2}{2\pi^2} \vec{E} \cdot \vec{\mathcal{B}}, \tag{A3}$$

where J_5^μ is the density of the axial current. In the integral form the same equation can be written as

$$\frac{dQ_5}{dt} = 2 \int_V \frac{e^2}{4\pi^2} \vec{E} \cdot \vec{\mathcal{B}} \, dV \quad \text{where} \quad Q_5 \equiv \int_V J_5^0 \, dV, \tag{A4}$$

---

[11]In particle physics literature the magnetic helicity is defined with additional coefficient $e^2/(4\pi^2)$ in front of the integral (A1). This normalization factor becomes obvious from Eq. (A5).

[12]An important observation here is that the integrand entering (A2) which describes the dissipation of the magnetic helicity $\mathcal{H}$ identically vanishes in ideal MHD where $\vec{E} = -\vec{v} \times \vec{\mathcal{B}}$.

where the surface term has been ignored. Comparing (A2) and (A4) one arrives at the following result (see e.g. review papers [60,61] on the subject)

$$\frac{d}{dt}\left(Q_5 + \frac{e^2}{4\pi^2}\mathcal{H}\right) = 0, \qquad (A5)$$

which implies that the magnetic helicity (A1) in combination with the axial charge (A4) becomes a conserved quantity, while they are not conserved separately. An important element to note here is that the axial current is the combination of right- and left-handed currents, i.e. $J_5^\mu = J_R^\mu - J_L^\mu$, while μ_5 is the chemical potential for J_5^μ. The significance of μ_5 is explained in item 12 in Sec. VII. One comment here is that $\mu_5 \neq 0$ is not a true chemical potential as it is not associated with any exactly conserved charges (in contrast with μ which corresponds to the conserved baryon charge).

The significance of Eq. (A5) is that the Q_5 and $\mathcal{H}$ are strongly coupled with each other such that the decrease of Q_5 will lead to an increase of $\mathcal{H}$ and vice versa. This implies that the magnetic helicity $\mathcal{H}$ can be refilled and restored (in principle) after the reconnection, and the source of the refill of the magnetic helicity $\mathcal{H}$ is the chiral charge Q_5 determined by parameter μ_5.

Now we want to make several comments on the currents and their properties which could generate the chiral asymmetry and consequently the magnetic helicity $\mathcal{H}$, which obviously belong to the class of topological effects. Normally, the topological phenomena are also associated with the topological features of the sources, such as nondissipating currents. A well-known example of such a relation is the quantization of the magnetic flux and associated with the quantized flux the nondissipating supercurrent.

It is very instructive to explain the differences between the currents by analyzing their symmetric properties. We start with analysis of the conventional Ohm's law

$$\vec{J}^{\text{ohm}} = \sigma\vec{E}, \qquad (A6)$$

where σ is the Ohmic conductivity. Both electric current $\vec{J}$ and electric field $\vec{E}$ are normal vectors ($\mathcal{P}$ odd) under $\mathcal{P}$ symmetry. Therefore, the σ has to be $\mathcal{P}$ even. If we consider the time reversal symmetry $\mathcal{T}: t \to -t$ we observe that the current $\vec{J}^{\text{ohm}}$ is $\mathcal{T}$ odd, while the electric field $\vec{E} = -\vec{\nabla}V$ is $\mathcal{T}$ even. Therefore, the Ohmic conductivity σ has to be odd under the $\mathcal{T}$ reversal for Ohm's law (A6) to make sense. This is an anticipated result since the Ohmic conductivity describes processes of dissipation that produce entropy, and entropy production by the second law of thermodynamics is an irreversible process which generates an arrow of time. In fact, all conventional transport coefficients are odd under $\mathcal{T}$ reversal being consistent with the presented argument.

Now we consider the so-called chiral magnetic effect (CME) when the electric current is induced due to the chiral asymmetry expressed in terms of the chemical potential μ_5 (see reviews [60,61]):

$$\vec{J}^{\text{top}} = \sigma_5\vec{\mathcal{B}}, \qquad \sigma_5 = \frac{e^2}{2\pi^2}\mu_5. \qquad (A7)$$

The difference with the previous case of Ohm's law (A6) is that the magnetic field $\vec{\mathcal{B}} = \vec{\nabla} \times \vec{\mathcal{A}}$ is $\mathcal{T}$ odd because the vector potential $\vec{\mathcal{A}}$ is $\mathcal{T}$ odd. From (A7) we infer that σ_5 has to be $\mathcal{T}$ even, and the topological current $\vec{J}^{\text{top}}$ entering (A7) is expected to be nondissipating.

It is very instructive to compare this analysis with another type of nondissipating current which is induced in superconducting materials. This is also important from a phenomenological viewpoint as the NS is believed to be a large superconductor.[13] The corresponding physics is captured by the London relation between the electric current and gauge potential

$$\vec{J}^{\text{London}} = \lambda^{-2}\vec{\mathcal{A}}, \qquad \vec{\nabla} \cdot \vec{\mathcal{A}} = 0, \qquad (A8)$$

where λ is the penetration length. The vector potential $\vec{\mathcal{A}}$ as well as $\vec{J}^{\text{London}}$ are $\mathcal{T}$ odd functions, which suggests that the London current $\vec{J}^{\text{London}}$ is nondissipating. Indeed, the magnetic flux through an Abrikosov vortex for type II superconductor is quantized. This means that the circulating supercurrent is topologically protected—it is not allowed to dissipate as the flux is quantized.

The nondissipating nature of the topological current (A7) is also supported by analysis [58] where it has been argued that the conventional $\mathcal{P}$- and $\mathcal{T}$-even QED processes (which are normally incorporated in MHD analyses) cannot eliminate the current (A7). Indeed, the correlation $\langle\vec{J}^{\text{top}} \cdot \vec{\mathcal{B}}\rangle$ is a $\mathcal{P}$-odd correlation which cannot be changed by conventional $\mathcal{P}$-even QED processes.[14] The $\mathcal{P}$-odd weak interactions are capable of diminishing the induced current (A7) which was generated by weak interactions when the NS's temperature was sufficiently high; see [58] for details. The surface effects can also play a role as helicity may leak through the surface. However, these surface effects are expected to be subdominant, and not considered here.

We finish this appendix with an order of magnitude estimate of the total energy reservoir which potentially can

---

[13]It remains to be a matter of debate whether superconductivity realized in NSs is a type I or type II superconductor [75].

[14]We emphasize that the claim is not that the transitions $L \to R$ and $R \to L$ do not occur all the time. These transitions of course occur in QED as for example, the mass term flips the chirality. The claim is that the expectation value $\langle\vec{J}^{\text{top}} \cdot \vec{\mathcal{B}}\rangle$ in equilibrium (including the magnetic portion of the helicity $\mathcal{H}$) cannot be washed out without $\mathcal{P}$-odd weak interactions.

refill the magnetic helicity. As we mentioned after (A5) the strength of helicity $\mathcal{H}$ can be restored after every event of reconnection by conversion of the energy from Q_5. By definition, $J_5^0 = \int_V (J_R^0 - J_L^0)\, dV$ is the difference between right- and left-handed densities. The source of this asymmetry is μ_5, which was estimated in [58]. The most important parameters for the present estimate from [58] is the asymmetry parameter P_{asym} and the Fermi momenta $k_e \sim \mu$ for electrons numerically assume the following values:

$$P_{\text{asym}} \sim \frac{\mu_5}{\mu} \approx 2 \times 10^{-5}, \qquad \mu \approx 100 \text{ MeV}. \quad \text{(A9)}$$

From (A9) one can estimate the total difference between right- and left-handed electrons in the entire NS as follows:

$$\left(\frac{\mu_R^3}{3\pi^2} - \frac{\mu_L^3}{3\pi^2} \right) \left(\frac{4\pi R^3}{3} \right) \approx \frac{\mu^2 \mu_5}{\pi^2} \left(\frac{4\pi R^3}{3} \right) \sim 10^{51}. \quad \text{(A10)}$$

The total energy reservoir which is available to refill the magnetic helicity $\mathcal{H}$ can be estimated as follows. One should multiply Eq. (A10) to a typical energy of electrons, which is determined by μ. Therefore, we arrive at the following estimate for the total available energy:

$$E_{(R-L)}^{\text{tot}} \sim \mu \cdot \left(\frac{\mu^2 \mu_5}{\pi^2} \right) \cdot \left(\frac{4\pi R^3}{3} \right) \sim 10^{47} \text{ erg.} \quad \text{(A11)}$$

It is instructive to compare this total energy (produced at early times due to the generation of the right-left asymmetry) with total magnetic energy as given by (28). It is clear that the total energy reservoir (A11) is enormous. This amount of energy is more than sufficient to refill the magnetic helicity $\mathcal{H}$ after each magnetic reconnection to heat the NS's surface, which is precisely the proposal mentioned in items 11–14 in Sec. VII. As we mentioned above this asymmetry cannot be washed out by conventional QED $\mathcal{P}$-even processes incorporated into MHD. Only the $\mathcal{P}$-odd weak interactions are capable of diminishing this asymmetry. But these processes are very slow at low temperatures [58], and unlikely to play a role.

APPENDIX B: RADIO BANDS AS INDICATOR OF THE MAGNETIC RECONNECTION

It is known that the magnetic reconnection is also accompanied by emission in radio frequency bands as the solar flare observations suggest. Therefore, one could expect that the search in radio frequency bands could be an alternative way to study the heating mechanism due to the magnetic reconnection in NSs along with x ray as suggested in Sec. VIII. The main goal of this appendix is to make an order of magnitude estimate for the expected radio signal from NSs which accompanies the magnetic reconnection. We follow the same logic in these estimates as we used previously for the x ray analysis in Sec. VIII.

It is known that along with x rays there is another indicator for solar flares, the so-called $F_{10.7}$ flux which reflects the solar activity in a radio wave band with wave length 10.7 cm. Typical enhancement during the solar flare is about 200 sfu (solar flux units); see Fig 2 in Ref. [54]. Converting sfu to conventional units we arrive at the following estimate for the radio emission during the solar flare,

$$\langle F_{\text{radio}}^{\odot} \rangle \approx 6 \times 10^{-8} \; \frac{\text{erg}}{\text{s} \cdot \text{cm}^2}, \qquad \text{sfu} \equiv 10^{-22} \; \frac{\text{W}}{\text{m}^2 \, \text{Hz}}$$

$$\xi_{\text{radio}}^{2.7 \text{ GHz}} \equiv \frac{\langle F_{\text{radio}}^{\odot} \rangle}{\langle F_X^{\odot} \rangle} \approx 6 \times 10^{-6}. \quad \text{(B1)}$$

We assume that this ratio ξ_{radio} holds for NSs as well. Therefore, assuming the flat spectrum we arrive at the following estimate for $\langle F_{\text{radio}}^{\text{NS}} \rangle$:

$$\langle F_{\text{radio}}^{\text{NS}} \rangle \sim \xi_{\text{radio}}^{1.4 \text{ GHz}} \cdot \langle F_X^{\text{NS}} \rangle$$

$$\sim 3 \cdot (10^{-19} - 10^{-20}) \left(\frac{T_s}{10^6 \text{ K}} \right)^4 \left(\frac{0.1 \text{ kpc}}{r} \right)^2 \frac{\text{erg}}{\text{s} \cdot \text{cm}^2}, \quad \text{(B2)}$$

where we use our estimate for $\langle F_X^{\text{NS}} \rangle$ from (38).

It is instructive to present a numerical value of the flux $\langle F_{\text{radio}}^{J1856} \rangle$ for $J1856$ from M7 stars where x-ray flux is recorded according to Eq. (40),

$$\langle F_{\text{radio},1.4 \text{ GHz}}^{J1856} \rangle \sim 4 \times 10^{-21} \; \frac{\text{erg}}{\text{s} \cdot \text{cm}^2}, \quad [\text{prediction}], \quad \text{(B3)}$$

while the observed upper limit for this star in 1.4 GHz band is $10^{-4} \, (\text{mJy}) \, (\text{kpc}^2)$, which is almost 2 orders of magnitude higher than (B3); see Fig. 14 in [63]. Therefore, we are not optimistic with possible observations of the radio signals from NSs which always accompany the magnetic reconnection, but we are quite optimistic with possible observations in a hard x-ray energy band as discussed in the main body of the text in Sec. VIII.

[1] C. Kouvaris, Phys. Rev. D **77,** 023006 (2008).
[2] C. Kouvaris and P. Tinyakov, Phys. Rev. D **82,** 063531 (2010).
[3] A. de Lavallaz and M. Fairbairn, Phys. Rev. D **81,** 123521 (2010).
[4] C. Kouvaris and P. Tinyakov, Phys. Rev. D **83,** 083512 (2011).
[5] S. D. McDermott, H.-B. Yu, and K. M. Zurek, Phys. Rev. D **85,** 023519 (2012).
[6] N. F. Bell, A. Melatos, and K. Petraki, Phys. Rev. D **87,** 123507 (2013).
[7] J. Bramante, K. Fukushima, J. Kumar, and E. Stopnitzky, Phys. Rev. D **89,** 015010 (2014).
[8] J. Bramante and T. Linden, Phys. Rev. Lett. **113,** 191301 (2014).
[9] J. Bramante, A. Delgado, and A. Martin, Phys. Rev. D **96,** 063002 (2017).
[10] M. Baryakhtar, J. Bramante, S. W. Li, T. Linden, and N. Raj, Phys. Rev. Lett. **119,** 131801 (2017).
[11] J. Bramante, T. Linden, and Y.-D. Tsai, Phys. Rev. D **97,** 055016 (2018).
[12] N. Raj, P. Tanedo, and H.-B. Yu, Phys. Rev. D **97,** 043006 (2018).
[13] S. Chatterjee, R. Garani, R. K. Jain, B. Kanodia, M. S. N. Kumar, and S. K. Vempati, Phys. Rev. D **108,** L021301 (2023).
[14] S. Bhattacharya, B. Dasgupta, R. Laha, and A. Ray, Phys. Rev. Lett. **131,** 091401 (2023).
[15] J. Bramante and N. Raj, Phys. Rep. **1052,** 1 (2024).
[16] M. S. Turner, Annu. Rev. Nucl. Part. Sci. **72,** 1 (2022).
[17] G. Bertone and D. Hooper, Rev. Mod. Phys. **90,** 045002 (2018).
[18] E. Witten, Phys. Rev. D **30,** 272 (1984).
[19] E. Farhi and R. L. Jaffe, Phys. Rev. D **30,** 2379 (1984).
[20] A. De Rujula and S. L. Glashow, Nature (London) **312,** 734 (1984).
[21] D. G. Yakovlev and C. J. Pethick, Annu. Rev. Astron. Astrophys. **42,** 169 (2004).
[22] D. Gonzalez and A. Reisenegger, Astron. Astrophys. **522,** A16 (2010).
[23] K. Yanagi, N. Nagata, and K. Hamaguchi, Mon. Not. R. Astron. Soc. **492,** 5508 (2020).
[24] F. Köpp, J. E. Horvath, D. Hadjimichef, C. A. Z. Vasconcellos, and P. O. Hess, Int. J. Mod. Phys. D **32,** 2350046 (2023).
[25] A. R. Zhitnitsky, J. Cosmol. Astropart. Phys. 10 (2003) 010.
[26] X. Liang and A. Zhitnitsky, Phys. Rev. D **94,** 083502 (2016).
[27] S. Ge, X. Liang, and A. Zhitnitsky, Phys. Rev. D **96,** 063514 (2017).
[28] S. Ge, X. Liang, and A. Zhitnitsky, Phys. Rev. D **97,** 043008 (2018).
[29] S. Ge, K. Lawson, and A. Zhitnitsky, Phys. Rev. D **99,** 116017 (2019).
[30] A. Zhitnitsky, Mod. Phys. Lett. A **36,** 2130017 (2021).
[31] J. Singh Sidhu, R. J. Scherrer, and G. Starkman, Phys. Lett. B **807,** 135574 (2020).
[32] O. P. Santillán and A. Morano, Phys. Rev. D **104,** 083530 (2021).

[33] D. Budker, V. V. Flambaum, and A. Zhitnitsky, Symmetry **14,** 459 (2022).
[34] A. Zhitnitsky, Phys. Rev. D **74,** 043515 (2006).
[35] V. V. Flambaum and A. R. Zhitnitsky, Phys. Rev. D **99,** 023517 (2019).
[36] K. Lawson and A. R. Zhitnitsky, Phys. Dark Universe **24,** 100295 (2019).
[37] A. Zhitnitsky, J. Phys. G **49,** 105201 (2022).
[38] M. M. Forbes and A. R. Zhitnitsky, Phys. Rev. D **78,** 083505 (2008).
[39] A. Zhitnitsky, J. Cosmol. Astropart. Phys. 10 (2017) 050.
[40] A. Zhitnitsky, Phys. Dark Universe **22,** 1 (2018).
[41] N. Raza, L. van Waerbeke, and A. Zhitnitsky, Phys. Rev. D **98,** 103527 (2018).
[42] S. Ge, M. S. R. Siddiqui, L. Van Waerbeke, and A. Zhitnitsky, Phys. Rev. D **102,** 123021 (2020).
[43] E. N. Parker, Astrophys. J. **330,** 474 (1988).
[44] S. Krucker and A. O. Benz, Sol. Phys. **191,** 341 (2000).
[45] A. O. Benz and S. Krucker, IAU Symp. **203,** 471 (2001).
[46] U. Mitra-Kraev and A. O. Benz, Astron. Astrophys. **373,** 318 (2001).
[47] A. O. Benz and S. Krucker, Astrophys. J. **568,** 413 (2002).
[48] A. O. Benz and P. C. Grigis, Adv. Space Res. **32,** 1035 (2003).
[49] J. A. Klimchuk, Sol. Phys. **234,** 41 (2006).
[50] J. A. Klimchuk, arXiv:1709.07320.
[51] S. Bertolucci, K. Zioutas, S. Hofmann, and M. Maroudas, Phys. Dark Universe **17,** 13 (2017).
[52] L. van Waerbeke and A. Zhitnitsky, Phys. Rev. D **99,** 043535 (2019).
[53] L. D. Landau and E. M. Lifshitz, *The Classical Theory of Fields*, 4th ed. (Butterworth-Heinemann, Oxford, 1975).
[54] E. A. Bruevich and G. V. Yakunina, Astrophysics (Engl. Transl.) **60,** 387 (2017).
[55] P. Kumar, W. Lu, and M. Bhattacharya, Mon. Not. R. Astron. Soc. **468,** 2726 (2017).
[56] B. Zhang, Rev. Mod. Phys. **95,** 035005 (2023).
[57] D. Li et al., Nature (London) **598,** 267 (2021).
[58] J. Charbonneau and A. Zhitnitsky, J. Cosmol. Astropart. Phys. 08 (2010) 010.
[59] D. Kharzeev and A. Zhitnitsky, Nucl. Phys. A **797,** 67 (2007).
[60] D. E. Kharzeev, Ann. Phys. (Amsterdam) **325,** 205 (2010).
[61] D. E. Kharzeev, J. Liao, S. A. Voloshin, and G. Wang, Prog. Part. Nucl. Phys. **88,** 1 (2016).
[62] D. Page, U. Geppert, and M. Kueker, Astrophys. Space Sci. **308,** 403 (2007).
[63] C. Dessert, J. W. Foster, and B. R. Safdi, Astrophys. J. **904,** 42 (2020).
[64] G. G. Pavlov, O. Kargaltsev, J. A. Wong, and G. P. Garmire, Astrophys. J. **691,** 458 (2009).
[65] A. P. Igoshev, S. B. Popov, and R. Hollerbach, Universe **7,** 351 (2021).
[66] S. Tulin and H.-B. Yu, Phys. Rep. **730,** 1 (2018).
[67] A. Zhitnitsky, Phys. Dark Universe **40,** 101217 (2023).
[68] R. C. Henry, J. Murthy, J. Overduin, and J. Tyler, Astrophys. J. **798,** 14 (2014).
[69] M. S. Akshaya, J. Murthy, S. Ravichandran, R. C. Henry, and J. Overduin, Astrophys. J. **858,** 101 (2018).

[70] M. S. Akshaya, J. Murthy, S. Ravichandran, R. C. Henry, and J. Overduin, Mon. Not. R. Astron. Soc. **489**, 1120 (2019).

[71] A. Zhitnitsky, Phys. Lett. B **828**, 137015 (2022).

[72] A. R. Choudhuri, *Philosophy and Foundations of Physics* (Cambridge University Press, Cambridge, England, 1998).

[73] E. Pariat, G. Valori, P. Démoulin, and K. Dalmasse, Astron. Astrophys. **580**, A128 (2015).

[74] S. Yang, J. Buechner, J. Skala, and H. Zhang, Astron. Astrophys. **613**, A27 (2018).

[75] K. B. W. Buckley, M. A. Metlitski, and A. R. Zhitnitsky, Phys. Rev. Lett. **92**, 151102 (2004).